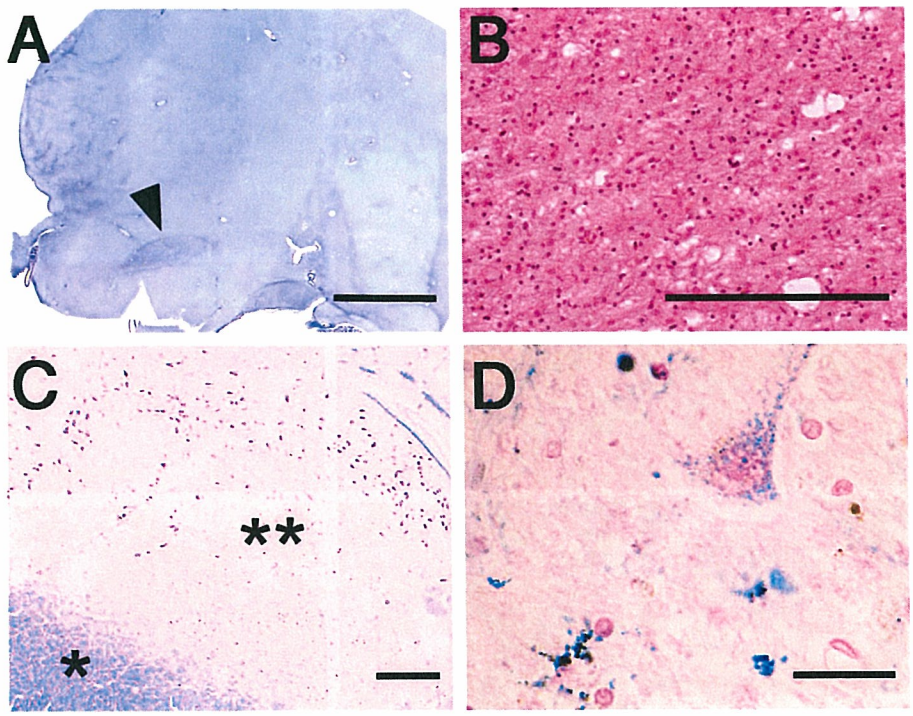

Fig. 3 A: Fibrillary gliosis is the subthalamic nucleus (arrowhead) (Holzer). Bar; 1mm. B: Moderate neuronal loss with marked gliosis in the subthalamic nucleus (HE). Bar; 250 µm. C: Mild neuronal loss in the medial part of the substantia nigra (double asterisk). Cerebral peduncle (asterisk) (KB). Bar; 400 µm. D: Iron deposition in the neurons and astrocytes of the substantia nigra (Berlin blue). Bar; 30 µm.

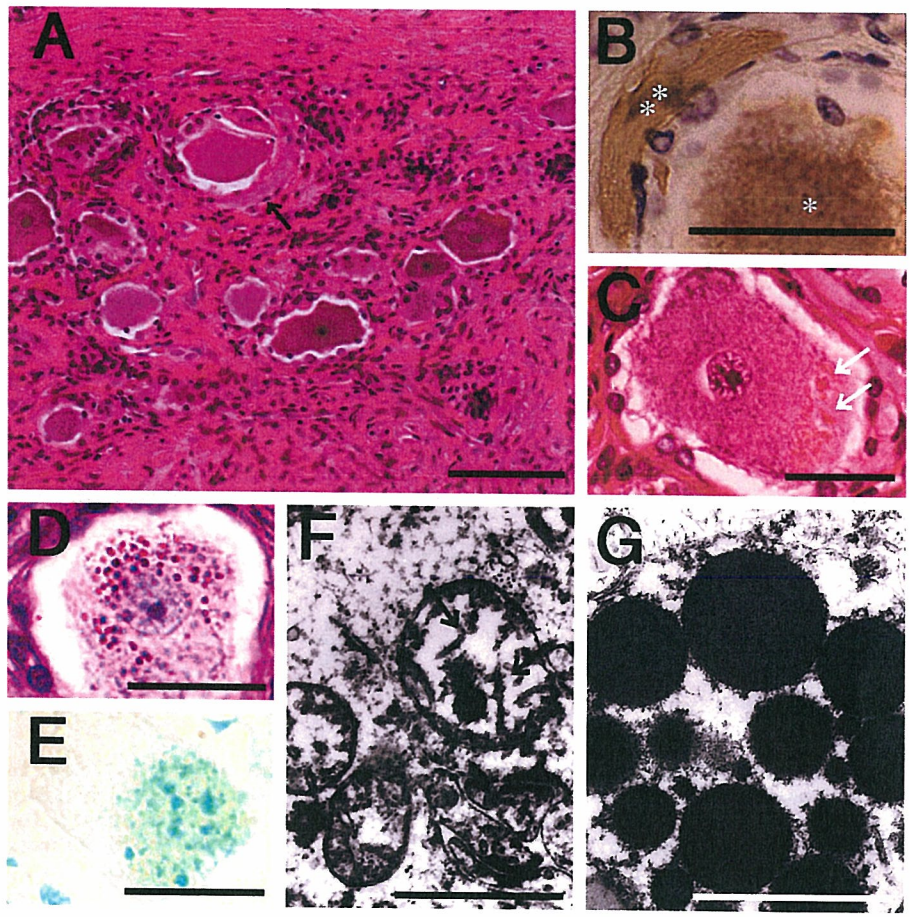

Fig. 4 A: Degeneration of the cervical spinal ganglion. Scattered Nageott□fs residual nodules with loss of neurons. Arrow indicates swollen axon (HE). Bar; 100 µm. B: A neuron (asterisk) in a dorsal root ganglion at the 7th cervical segment with axonal swelling (double asterisk) (immunohistochemistry for neurofilament). Bar; 50 µm. C: Acidophilic granules in a neuron of the dorsal root ganglion (arrows) (HE). Bar; 50 µm. D, E: Acidophilic granules in the spinal ganglion positive for periodic-acid Schiff (D), and luxol fast blue (E) staining. Bar; 30 µm. F: Ultrastructure of acidophilic granules in the lumbar spinal ganglia. Amorphous and globular bodies of homogeneous material, and surrounded by a double-layered limiting membrane. Mitochondrial cristae (arrows) are evident. Bar; 1µm. G: Surface of the bodies is thorny (F-G, Uranyl acetate and lead citrate). Bar; 1µm.

Brain Advance Access published April 17, 2007

doi:10.1093/brain/awm065

TDP-43 is deposited in the Guam parkinsonism–dementia complex brains

Masato Hasegawa,[1,*] Tetsuaki Arai,[2,*] Haruhiko Akiyama,[2] Takashi Nonaka,[1] Hiroshi Mori,[3] Tomoyo Hashimoto,[4] Mineo Yamazaki[4] and Kiyomitsu Oyanagi[4]

[1]Departments of Molecular Neurobiology and [2]Psychogeriatrics, Tokyo Institute of Psychiatry, Tokyo Metropolitan Organization for Medical Research, 2-1-8 Kamikitazawa, Setagaya-ku, Tokyo 156-8585, [3]Department of Neuroscience, Osaka City University School of Medicine, 1-4-3 Asahimachi, Abenoku, Osaka 545-8585 and [4]Department of Neuropathology, Tokyo Metropolitan Institute for Neuroscience, Tokyo Metropolitan Organization for Medical Research, 2-6 Musashidai, Fuchu, Tokyo 183-8526, Japan

*These authors contributed equally to this work.

Correspondence to: Masato Hasegawa and Tetsuaki Arai, Tokyo Institute of Psychiatry, Tokyo Metropolitan Organization for Medical Research, 2-1-8 Kamikitazawa, Setagaya-ku, Tokyo 156-8585, Japan
E-mail: masato@prit.go.jp

TDP-43, a nuclear factor that functions in regulating transcription and alternative splicing, was recently identified as a component of the ubiquitin-positive, tau-negative inclusions specific for frontotemporal lobar degeneration (FTLD-U) and amyotrophic lateral sclerosis (ALS). In the present study, we carried out immunohistochemical and biochemical analyses of brains of Guamanians with the parkinsonism–dementia complex (G-PDC) using anti-TDP-43, anti-tau and anti-ubiquitin antibodies. Immunohistochemistry with anti-TDP-43 antibodies revealed various types of positive structures in the frontotemporal and hippocampal regions of G-PDC cases. Most of these structures were negative for tau. By immunoblot analysis with the TDP-43 antibody, an abnormal 45 kDa band, as well as a diffuse staining throughout the gel, was detected in the sarkosyl-insoluble fractions of G-PDC brains. Dephosphorylation has shown that abnormal phosphorylation takes place in the accumulated TDP-43 seen in FTLD-U and ALS. These results suggest that accumulation of TDP-43 is a common process in certain neurodegenerative disorders, including FTLD-U, ALS and G-PDC.

Keywords: frontotemporal lobar degeneration; amyotrophic lateral sclerosis; ubiquitin; tau; inclusion

Abbreviations: ALS = amyotrophic lateral sclerosis; FTLD-U = frontotemporal lobar degeneration; G-PDC = Guam parkinsonism–dementia complex; NCI = neuronal cytoplasmic inclusions; NII = neuronal intranuclear inclusions

Received January 29, 2007. Revised March 7, 2007. Accepted March 8, 2007

Introduction

Ubiquitin-positive, tau-negative neuronal cytoplasmic inclusions (NCI) were first described in patients with amyotrophic lateral sclerosis (ALS) (Okamoto *et al.*, 1991). They were subsequently found in patients with frontotemporal lobar degeneration with motor neuron disease (FTLD-MND) (Okamoto *et al.*, 1992; Wightman *et al.*, 1992), and FTLD with MND-type inclusions but without MND (FTLD-MND-type) (Bergmann *et al.*, 1996; Jackson *et al.*, 1996; Iseki *et al.*, 1998). FTLD-MND and FTLD-MND-type are referred to as FTLD-U (Mackenzie *et al.*, 2006*a*). In some FTLD-U cases, neuronal intranuclear inclusions (NII) have been described (Woulfe *et al.*, 2001; Mackenzie and Feldman, 2003, 2005; Forman *et al.*, 2006), especially in those cases with autosomal dominant inheritance associated with mutations in progranulin gene (Baker *et al.*, 2006; Boeve *et al.*, 2006; Cruts *et al.*, 2006; Gass *et al.*, 2006; Huey *et al.*, 2006; Mackenzie *et al.*, 2006*b*; Masellis *et al.*, 2006; Mukherjee *et al.*, 2006; Pickering-Brown *et al.*, 2006; Snowden *et al.*, 2006) and in valosin-containing protein gene (Guyant-Marechal *et al.*, 2006). Recently, TDP-43, a ubiquitously expressed nuclear protein, was identified as the major component of the ubiquitin-positive inclusions in these disorders (Arai *et al.*, 2006; Neumann *et al.*, 2006, 2007; Davidson *et al.*, 2007). They include NCI, NII and dystrophic neurites in the hippocampus and frontotemporal cortex in cases of FTLD-U, and skein-like inclusions in the spinal cord in FTLD-MND and ALS cases.

The Guam parkinsonism–dementia complex (G-PDC) and amyotrophic lateral sclerosis (G-ALS) are neurodegenerative disorders of Chamorro residents of Guam. They are clinically characterized by either progressive cognitive impairment with extrapyramidal signs or motor neuron dysfunctions. G-PDC is characterized by severe neuronal loss and abundant neurofibrillary tangles (NFTs) in the temporal and frontal cortex, basal ganglia, thalamus and brainstem with a virtual absence of senile plaques (Hirano *et al.*, 1961; Nakano and Hirano, 1983; Oyanagi *et al.*, 1994*a*). Although environmental factors such as toxins in cycad seeds and minerals in the soils and drinking water have been implicated (Cox *et al.*, 2003; Hermosura *et al.*, 2005; Oyanagi *et al.*, 2006), the aetiology and the pathogenesis remain unknown. G-PDC exhibits similarities to FTLD-U in terms of the frontotemporal atrophy and the occurrence of ubiquitin positive inclusions in the dentate gyrus (Oyanagi *et al.*, 1994*b*; Ikemoto *et al.*, 1997). In the present study, we show that various types of tau-negative, TDP-43-positive structures are present in G-PDC brains. Immunoblot analysis revealed that hyperphosphorylated TDP-43 is deposited in the sarkosyl-insoluble fractions of G-PDC brains. These results suggest that a common pathogenic mechanism through conformational changes in TDP-43 may be associated with the neurodegeneration in FTLD-U, ALS and G-PDC.

Materials and methods

Materials

Brains from six cases of clinically and neuropathologically diagnosed G-PDC, two Japanese cases with Alzheimer's disease (AD) and two non-PDC non-ALS Guamanian controls were employed in this biochemical and immunohistochemical studies. Paraffin-embedded sections from three other G-PDC cases were also used for immunohistochemistry. The age, sex, brain weight, brain regions examined and diagnosis are given in Table 1.

Immunohistochemical analysis

Small blocks of frontal regions were dissected at autopsy or from fresh frozen brain samples and fixed overnight in 10% formalin neutral buffer solution (Wako). Blocks were cut on a vibratome at 50 μm thickness. The free-floating sections were treated with 3% H_2O_2/methanol for 30 min to block the internal peroxidase and incubated in 0.5% Triton X-100/PBS for 30 min. After blocking with 10% calf serum/PBS, sections were immunostained overnight with two well-characterized antibodies to TDP-43: a polyclonal (10782-1-AP, ProteinTech Group Inc., Chicago, IL; 1 : 3000) and a monoclonal (2E2-D3, Abnova Corporation, Taipei, Taiwan; 1 : 1000). Two monoclonal antibodies to phosphorylated tau (AT8; Innogenetics, Gent, Belgium, 1 : 1000 and PHF-1; generous gift from Dr P. Davies, 1 : 2000), a polyclonal and a monoclonal antibody to ubiquitin [Z0458; Dako, Denmark; 1 : 3000 and DF2 (Mori *et al.*, 1987); 1 : 200], and a monoclonal antibody to GFAP (6F2, DakoCytomation, Glostrup, Denmark; 1 : 100) were also used. For analysis of unfixed materials, Triton-X-insoluble pellets prepared from frozen brains (see below) were smeared on PLL-coated slide glasses and used. For immunostaining of the hippocampal region from G-PDC cases, 10% formalin-fixed and paraffin-embedded blocks were sectioned at 6 μm and stained with 10782-1-AP (1 : 300) and 2E2-D3 (1 : 100). Following treatment with the appropriate secondary antibody, labelling was detected using the avidin-biotinylated HRP complex (ABC) system coupled with a diaminobenzidine reaction to yield a brown precipitate. Pretreatment of tissues by autoclaving in 10 mM sodium citrate buffer for 10 min at 120°C was needed for staining with 2E2-D3 in paraffin-embedded sections.

Double-label immunofluorescence was performed using FITC and TRITC conjugated secondary antibodies. The sections were examined with a confocal laser microscope (LSM5 PASCAL; Carl Zeiss MicroImaging gmbh, Jena, Germany).

Immunoblot analysis

The sarkosyl-insoluble fractions were prepared as described (Arai *et al.*, 2006) with slight modifications. Frozen temporal or frontal cortex (0.5 g) from six cases of G-PDC, two cases with AD and two controls were homogenized in 10 volumes (5 ml) of buffer A (10 mM Tris–HCl, pH 7.5 containing 1 mM EGTA, 10% sucrose and 0.8 M NaCl). After addition of another 5 ml of buffer A containing 2% Triton-X100, the homogenate was incubated for 30 min at 37°C and spun at 100 000 × *g* for 30 min at 25°C. The pellet was homogenized in 10 volume of buffer A containing 1% Sarkosyl, incubated for 30 min at 37°C and spun at 100 000 × *g* for 30 min at 25°C. The sarkosyl-insoluble pellet was homogenized in 4 volumes of buffer A containing 1% CHAPS and spun at 100 000 × *g* for 20 min.

Table 1 Description of the subjects

Case no.	Age	Sex	Brain weight (g)	Regions	Clinical diagnosis	Neuropathological diagnosis
1(CON1)	68	F	990	Frontal	Diabetes, heart failure	Normal-aged brain
2(CON2)	43	F	1370	Frontal	Burn	Slight edematous brain
3(G-PDC1)	69	F	1050	Frontal	PDC	PDC
4(G-PDC2)	69	M	875		PDC	PDC
5(G-PDC3)	52	F	1025	Frontal	PDC, myocardiac infarct	PDC
6(G-PDC4)	52	M	1025	Frontal	PDC	PDC
7(G-PDC5)	56	M	1235	Frontal	PDC, pneumonia	PDC
8(G-PDC6)	56	F	875	Frontal	PDC	PDC
9(G-PDC7)	51	F	850	Hip, temp	PDC	PDC
10(G-PDC8)	64	M	1290	Hip, Temp	PDC	PDC
11(G-PDC9)	57	F	1150	Hip, Temp	PDC	PDC
12(AD1)	82	F	670	Temp	AD	AD
13(AD2)	75	F	730	Temp	AD	AD

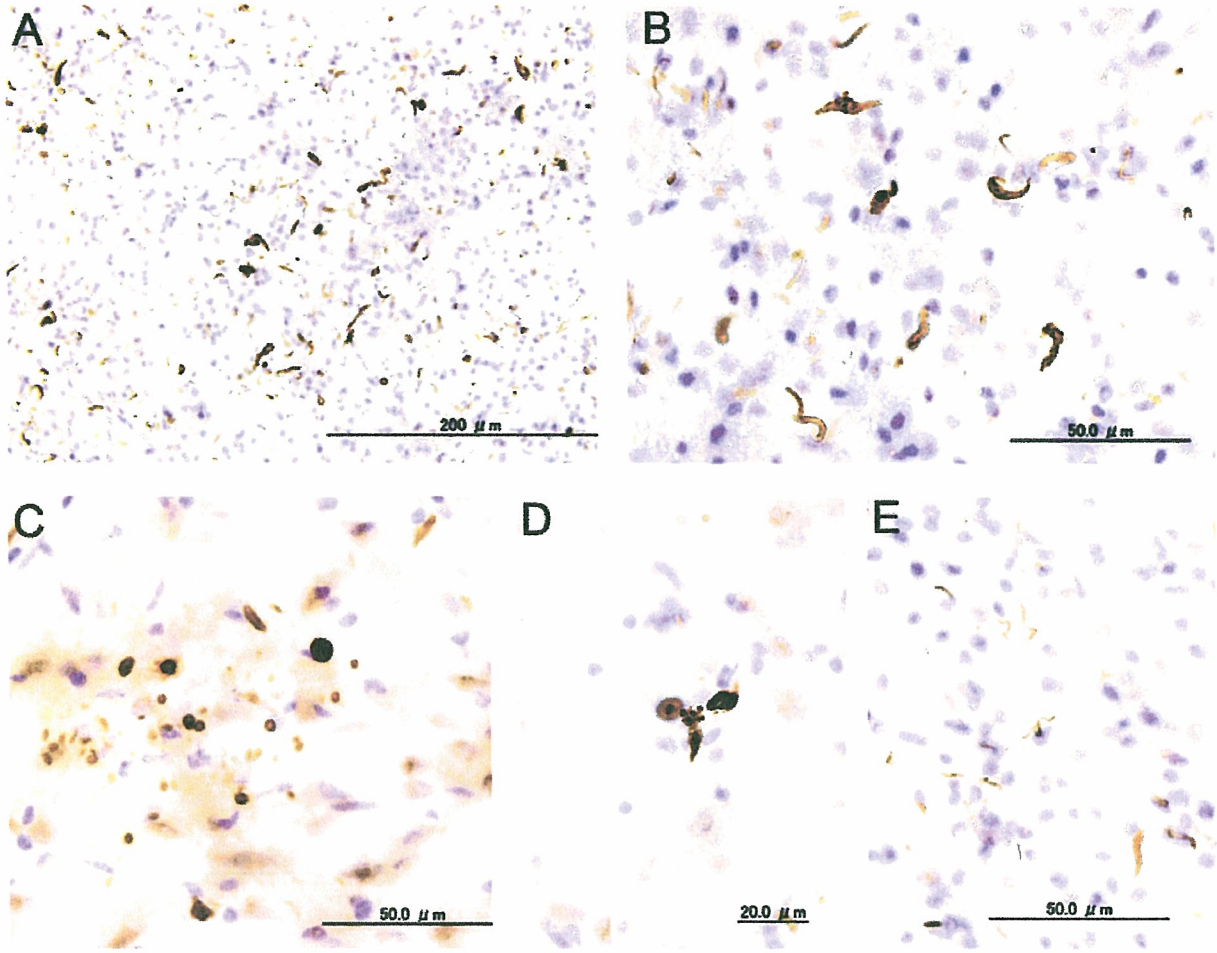

Fig. 1 Immunostainings of the frontal lobes of the G-PDC cases with the polyclonal antibody to TDP-43. **(A)** Numerous TDP-43 positive structures are observed in the white matter. **(B)** High magnification of coiled body-like or worm-like inclusions in the white matter. **(C)** Round-shape and dot-like TDP-43 positive structures in the grey matter. **(D)** Bud-shaped inclusions in the white matter. **(E)** Thin thread-like TDP-43 positive structures in the grey matter. The sections are counterstained with haematoxylin.

The pellet was sonicated in 0.8 volume of 7 M guanidine hydrochloride, dialysed against 30 mM Tris–HCl (pH 7.5), cleared by brief spin at 15 000 rpm and used for immunoblotting. For dephosphorylation, the sample was incubated with Lambda protein phosphatase as described (Arai *et al.*, 2006). For the analysis of proteins in white matter and grey matter, sarkosyl-insoluble proteins before and after dephosphorylation were prepared as described (Yamazaki *et al.*, 2005). Samples were run on SDS–PAGE using 10% polyacrylamide gel and the proteins were electrotransferred onto a polyvinylidene difluoride membrane, probed with the antibody to TDP-43, 10782-1-AP (1 : 3000) and the antibody to tau, HT7 (Innogenetics, Gent, Belgium; 1 : 3000), and detected as described (Arai *et al.*, 2006).

Results

Immunohistochemistry of G-PDC

Immunohistochemistry of G-PDC cases with the anti-TDP-43 antibodies revealed various types of inclusions. In vibratome sections of the frontal lobe, TDP-43 positive structures with various shapes (coiled-body-like, round-shape, dot-like, bud-shaped and thin thread-like) were present in both grey matter and white matter (Fig. 1A–E). These were similarly stained with both the polyclonal and monoclonal antibodies to TDP-43. The frequency of the inclusions varied from case to case, but they were detected in all six G-PDC cases examined. The number of TDP-43 positive structures in the white matter was much greater than that of ubiquitin positive ones in each G-PDC case. No such TDP-43-positive inclusions were observed on vibratome brain sections of the AD cases and the controls.

Various types of structures were also observed in paraffin sections of the hippocampal region of G-PDC cases (Fig. 2). In the granular cells of the dentate gyrus, numerous NCI (A, B) and a few NII (C) were positive for TDP-43. The nuclear staining for TDP-43 was reduced in neurons with cytoplasmic inclusions compared to that in non-affected

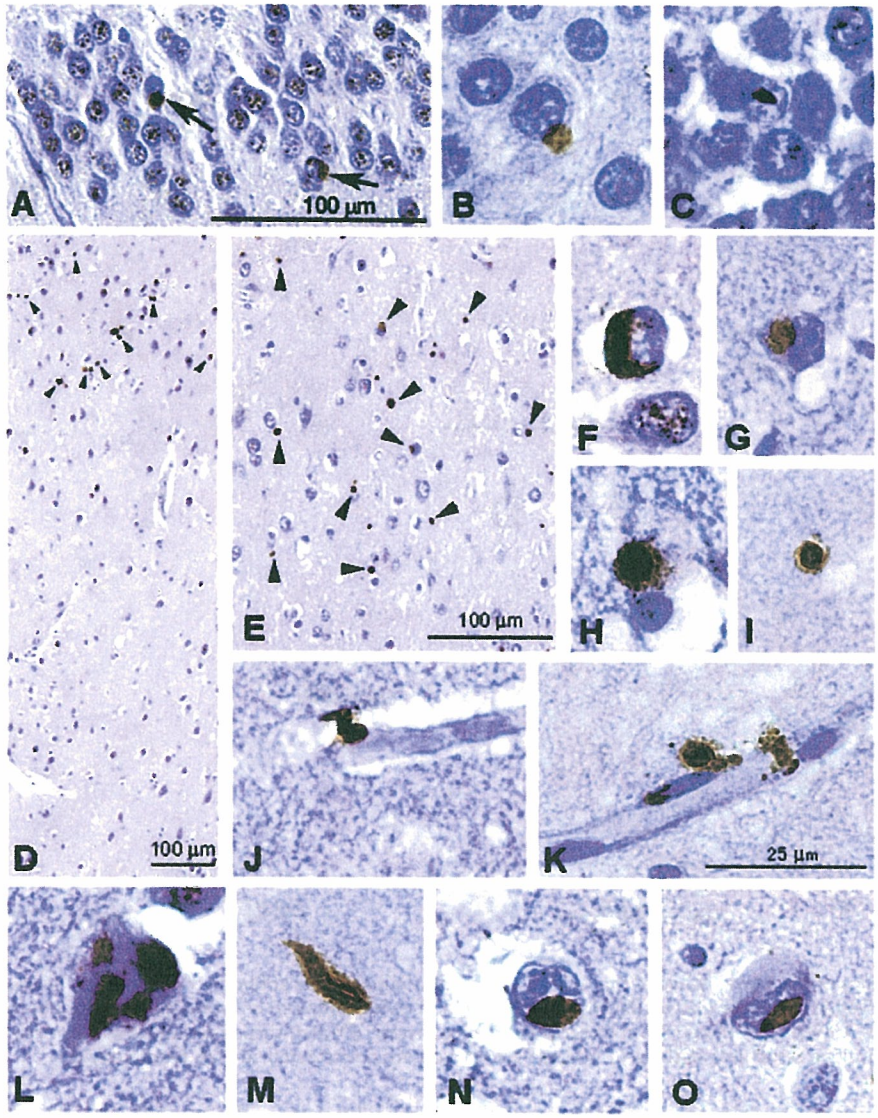

Fig. 2 Immunostainings of the hippocampus and the entorhinal cortex of the G-PDC cases. The polyclonal (**A**, **C**, **D**, **E**, **F**, **H**, **J**, **L** and **N**) and the monoclonal (**B**, **G**, **I**, **K**, **M** and **O**) antibodies to TDP-43 were used. In the granular cells of the dentate gyrus, frequent cytoplasmic inclusions with round or crescent shapes (arrows in **A**, **B**) and a few intranuclear inclusions (**C**) are observed. Note the absence of nuclear staining in neurons with cytoplasmic inclusions (arrows in **A**) compared to the granular staining of nuclei in nonaffected neurons. In the superficial layer of the entorhinal cortex, robust TDP-43 positive structures are seen (arrowheads in **D**, **E**). They include neuronal cytoplasmic inclusions (**F**, **G**), round structures (**H**, **I**), those associated with small blood vessels (**J**, **K**) or NFTs (**L**), the thread-like structure (**M**) and the intranuclear inclusions (**N**, **O**). The sections are counterstained with haematoxylin. Except for **A**, **D** and **E**, the same magnification is used as shown in **K**.

neurons as previously reported (Neumann *et al.*, 2006; Davidson *et al.*, 2007). In the parahippocampal cortex, TDP-43 positive structures tended to be more abundant in the superficial layer than in the deep layer (D, E). In addition to NCI (F, G), numerous round structures with similar size to glial nuclei were seen (H, I). There were also structures with round, dot-like or granular shape associated with small vessels (J, K). Occasional immunopositive structures associated with NFT were observed (L). Thread-like structures (M) and NII (N, O) were occasionally seen. All of these structures were positive for both the polyclonal and monoclonal antibodies to TDP-43, although the immunoreactivity was stronger with the polyclonal than with the monoclonal.

Nuclear TDP-43 staining varied much from case to case even in controls as previously reported (Davidson *et al.*, 2007). Furthermore, within cases showing TDP-43 nuclear staining, this was not evenly present in all nuclei, namely, a

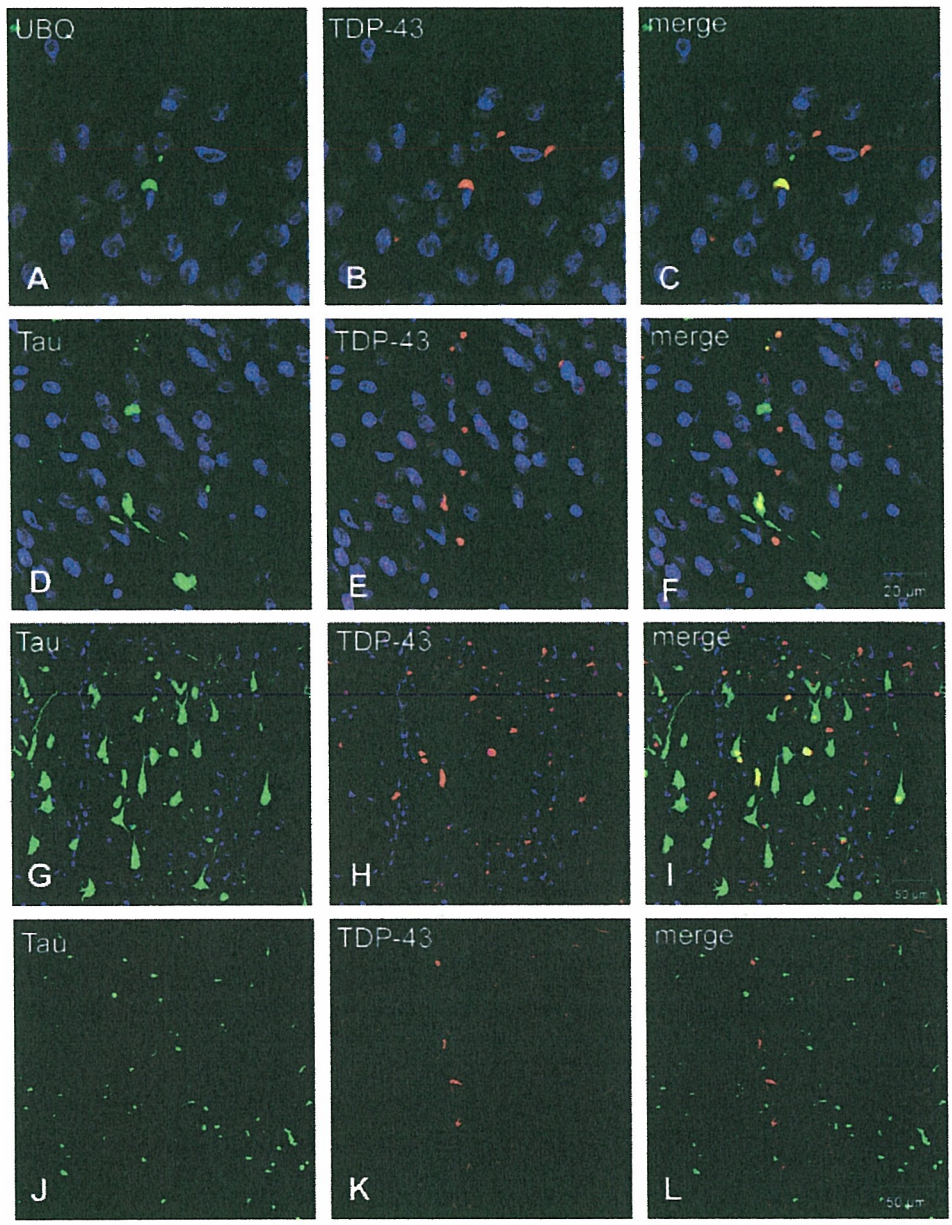

Fig. 3 Double-label immunofluorescence of the G-PDC cases with anti-ubiquitin (DF2 in **A**) or anti-tau (PHF-1 in **D** and **G**; AT8 in **J**) and anti-TDP-43 (**B**, **E**, **H** and **K**). Merged images are shown in **C**, **F**, **I** and **L**. In the granular cells in the dentate gyrus, a crescent inclusion shows colocalization (yellow fluorescence in **C**) of ubiquitin (green fluorescence in **A**) and TDP-43 (red fluorescence in **B**). Structures which are ubiquitin positive and TDP-43 negative (green in **C**) or ubiquitin negative and TDP-43 positive (red in **C**) are also observed. In the same region, colocalization of tau and TDP-43 are seen in some structures (yellow in **F**), but many TDP-43 positive structures are negative for tau (red in **F**). In the temporal cortex (**G**–**I**), most of the structures stained for tau (**G**) and those stained for TDP-43 (**H**) are independent, although colocalization of tau and TDP-43 is observed in part of NFTs (**I**). In the white matter of the frontal lobe, the distribution of structures positive for tau (**J**) and of those positive for TDP-43 (**K**) are virtually independent (**L**). In **A**–**I**, the cell nuclei are stained with TO-PRO-3 (Invitrogen, Tokyo, Japan), producing a blue colour. Scale bars are shown in **C**, **F**, **I** and **L**.

mix of TDP-43 positive and negative nuclei was seen (data not shown).

Figure 3 shows double immunofluorescence staining with anti-ubiquitin (A) or anti-tau (D, G and J) and anti-TDP-43 antibodies (B, E, H and K). Some NCI in the dentate gyrus were positive for both ubiquitin and TDP-43 (C). Most TDP-43 positive structures in the dentate gyrus and the temporal cortex were negative for tau, although

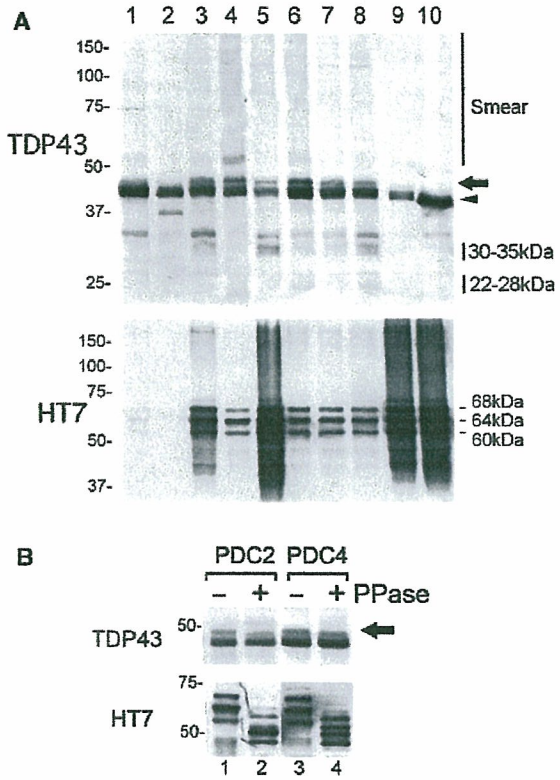

Fig. 4 Immunoblotting of the sarkosyl-insoluble fraction with anti-TDP-43 antibody (upper panel) and HT7 (lower panel). **(A)** Lanes 1 and 2, control (cases 1 and 2); lanes 3–8, G-PDC (cases 3–8); lanes 9 and 10, AD (cases 12 and 13). A positive band of 43 kDa (arrow head) is commonly seen in all cases, while an additional band of 45 kDa (arrow) as well as diffuse smear stainings are observed only in G-PDC brains (lanes 3–8). Several bands with 30–35 or 22–28 kDa are evident in five of six G-PDC cases (lanes 3, 5–8), although weak bands at 30–35 kDa are visible in a control case (lane 1) and in an AD case (lane 10). The triplet bands of 68, 64 and 60 kDa, typical for hyperphosphorylated tau in AD, and additional smear immunoreactivities are detected in all G-PDC cases examined. However, the intensities are much weaker than those found in two typical AD cases. **(B)** Immunoblotting of sarkosyl-insoluble fractions from the G-PDC cases before and after dephosphorylation. Partial mobility shift of the 45 kDa TDP-43-positive band (arrow) is observed after dephosphorylation of samples with lambda protein phosphatase. Mobility shifts in the PHF-tau bands are also detected with the HT7 antibody.

parts of NFTs were positive for TDP-43 (F, I). Virtually, no colocalization of tau and TDP-43 was observed in the white matter of the frontal lobe (L).

Immunoblot analysis of G-PDC

Figure 4 illustrates the results of immunoblotting of sarkosyl-insoluble fractions from two controls, six G-PDC cases and two AD cases with an anti-TDP-43 antibody or a phosphorylation independent anti-tau antibody HT7. By immunoblotting with HT7, the three major abnormal tau bands of 60, 64 and 68 kDa were detected in all G-PDC cases (Fig. 4A, lower panel). Although the pattern was indistinguishable to that seen in AD brains, the intensities of these tau bands in G-PDC cases were apparently weaker than those in two AD cases. By immunoblotting with the anti-TDP-43 antibody, a major band of 43 kDa corresponding to full-length TDP-43 was seen in all samples examined. In addition to the 43 kDa band, an abnormal 45 kDa band was observed in all G-PDC cases examined (lanes 3–8) which was not seen in the two controls (lanes 1 and 2) and two AD cases (lanes 9 and 10) (Fig. 4A, upper panel). Moreover, a diffuse smear staining was more prominent in G-PDC cases than in controls and AD cases (Fig. 4A, upper panel). Several positive bands of 30–35 or 22–26 kDa were evident in five of six G-PDC cases (lanes 3, 5–8), although faint bands at 30–35 kDa were visible in a control case (lane 1) and in an AD case (lane 10). After dephosphorylation of the samples with lambda protein phosphatase, a partial shift of the 45 kDa band was observed (Fig. 4B), suggesting that phosphorylation takes place in the full-length TDP-43. Similar results were obtained in the experiments with alkaline phosphatase at 37°C for 2 h (data not shown).

In order to confirm the deposition of TDP-43 in the white matter biochemically, the grey and white matters of two G-PDC cases were separated from each other macroscopically and the sarkosyl-insoluble fractions were immunoblotted with the anti-TDP-43 antibody. The abnormal 45 kDa band and smear stainings were detected in both the grey matter and the white matter (Fig. 5) and the intensities were slightly stronger in the sarkosyl-insoluble fractions from the white matter than in those from the grey matter in both cases (Fig. 5, upper panel). In contrast, immunoreactivities of tau bands detected with HT7 were much stronger in the grey matter than in the white matter in case PDC1 and similar deposits were detected in case PDC5 (Fig. 5, lower panel).

Discussion

TDP-43 is thought to function in transcriptional repression and exon skipping (Buratti *et al.*, 2001; Wang *et al.*, 2002; Ayala *et al.*, 2005; Buratti *et al.*, 2005). It was first identified as a protein capable of binding to a TAR DNA of the human immunodeficiency virus 1 (HIV-1) long terminal repeat region (Ou *et al.*, 1995). TDP-43 interacts with several nuclear ribonucleoproteins including heterogeneous nuclear RNP A/B and survival motor neuron protein, inhibiting alternative splicing (Wang *et al.*, 2002; Buratti *et al.*, 2005). The physiological function of TDP-43 in brain cells has not yet been determined. The present study showed numerous TDP-43 positive, tau-negative structures with various types of morphologies in white and grey matters of G-PDC brains.

Ubiquitin-positive inclusions have already been described in the granular cells of the hippocampal dentate gyrus in G-PDC cases. Most of these ubiquitin-positive inclusions

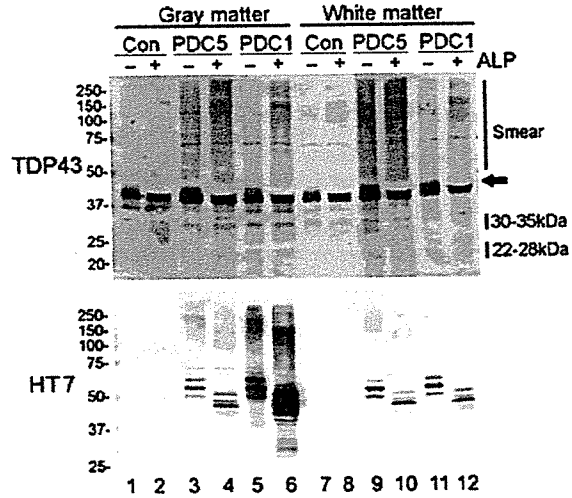

Fig. 5 Immunoblotting of the sarkosyl-insoluble fractions from grey or white matters of G-PDC cases with anti-TDP-43 antibody and HT7 before and after dephosphorylation. Lanes 1, 2, 7 and 8, control (case 2); lanes 3, 4, 9 and 10, G-PDC5 (case 7); lanes 5, 6, 11 and 12, G-PDC1 (case 3). Sarkosyl-insoluble fractions from grey matter (lanes 1–6) and white matter (lanes 7–12) before (lanes 1, 3, 5, 7, 9 and 11) and after (lanes 2, 4, 6, 8, 10 and 12) treatment with alkaline phosphatase (ALP) are immunoblotted with the TDP-43 antibody (upper panel) or HT7 (lower panel). The 45 kDa TDP-43 band (arrow) and the smeared stainings, which are not seen in control cases, are detected in both grey and white matter of the G-PDC cases. In both G-PDC cases, the intensities of the immunoreactivities for TDP-43 are stronger in the white matter than in the grey matter. In contrast, abundant tau is detected in the grey matter of the G-PDC1 case but less tau is observed in the white matter of G-PDC1 and in grey and white matter of G-PDC5 cases.

were reported to be tau-positive (Ikemoto *et al.*, 1997). In the present study, however, we showed that most of the TDP-43 positive inclusions in the granular cells in the hippocampus of G-PDC cases were negative for tau. These findings suggest that the occurrence of TDP-43 positive and tau negative neuronal inclusions in the hippocampus is common to FTLD-U, ALS and G-PDC. Some of the TDP-43-positive inclusions were also immunoreactive for ubiquitin, suggesting that partial ubiquitination may occur on the deposited TDP-43, as seen on tau in AD or α-synuclein in DLB.

On the other hand, the morphology and the distribution of some TDP-43 positive structures in the G-PDC cases seem to be different from those reported in FTLD-U cases (Arai *et al.*, 2006; Neumann *et al.*, 2006; Davidson *et al.*, 2007). For instances, in the frontal region, TDP-43 positive structures with various shapes were more pronounced in the white matter than in the grey matter in G-PDC cases, whereas NCI and dystrophic neurites were prominent in the superficial cortical layer in FTLD-U cases. The TDP-43 positive round structures (Fig. 2H and I) and those associated with small vessels (Fig. 2J and K) found in the parahippocampal and temporal cortices of G-PDC cases in this study have not so far been described in FTLD-U cases. These structures might not be considered corpora amylacea, based on the following points. First, the double immunofluorescence staining with antibodies to GFAP and TDP-43 showed that these TDP-43 positive structures were negative for GFAP (data not shown). Second, the laminar distribution of those was different from that of corpora amylacea, which is reported to be common in the surface glial feltwork in the outer part of layer I covering the cortex (Cavanagh, 1999). Finally, pretreatment of the section with 1 N KOH, which is reported to reduce the staining of corpora amylacea (Cavanagh, 1999), did not affect the staining of these structures with anti-TDP-43 antibodies (data not shown). It also seems unlikely that these TDP-43 positive round structures are normal nuclei since these are negative for haematoxylin (Fig. 2H–K) and for TO-PRO-3 (Fig. 3H). We speculate the possibility that these are degenerating nuclei or swollen processes like spheroids, but the nature of those should be further investigated.

The present biochemical studies demonstrate that hyperphosphorylated TDP-43 with a molecular weight of 45 kDa, fragments or splicing isoforms with lower molecular weight and the smearing substances with diffuse staining, similar to those found in FTLD-U and ALS, were deposited in the sarkosyl-insoluble fractions of G-PDC brains. The recovery of normal full-length TDP-43 in the sarkosyl-insoluble fraction might be due to its presence in the nucleus. These results suggest that accumulation of TDP-43 is a common process in certain neurodegenerative disorders, including ALS, FTLD-U and G-PDC, and similar biochemical alterations and conformational changes in TDP-43 may occur in these diseases.

It is unclear whether there are any relationships between the deposition of hyperphosphorylated tau and the accumulation of TDP-43. The occasional occurrence of TDP-43-positive structures associated with NFTs in the hippocampal and temporal regions of G-PDC cases may indicate some association between tau and TDP-43. However, it has to be noted that in a case of G-PDC (PDC3), the western blot of the sarkosyl insoluble fraction showed the most abundant tau (Fig. 4A, lower panel, lane 5) but the least amount of TDP-43 (Fig. 4A, upper panel, lane 5) among the all PDC cases examined. Although some unique tau positive structures, such as the granular hazy inclusions in astrocytes and the fine granules in white matter, have been previously reported in G-PDC (Oyanagi *et al.*, 1997; Yamazaki *et al.*, 2005), the association between these structures and TDP-43 was not examined in this study. Further studies will be needed to elucidate the role of the association between tau and TDP-43 in the pathogenesis of G-PDC.

There has been a long history of debate for the nosology of G-PDC. It is distinguished from AD by the laminar distribution of NFT (Hof *et al.*, 1991), the prominent glial pathology (Oyanagi *et al.*, 1997) and the relative absence of

amyloid plaques (Gentleman *et al.*, 1991; Schmidt *et al.*, 1998). The nature of α-synuclein pathology is also different between Parkinson's disease (PD) and G-PDC, i.e. the frequency of Lewy bodies in the substantia nigra is lower in G-PDC than in PD (Hirano *et al.*, 1966; Oyanagi and Wada, 1999), while the density of α-synuclein positive structures in the cerebellum is higher in G-PDC than in PD (Sebeo *et al.*, 2004). As for TDP-43, the predominance of white matter TDP-43 profiles is very unlike FTLD-U variants so far described. These findings suggest that G-PDC represents combined neurodegenerative disorders, in which tau, α-synuclein and TDP-43 are simultaneously involved, but does not represent mere co-existence of multiple common degenerative diseases, including AD, PD and FTLD-U.

In conclusion, the results of the present study suggest that a common pathogenic mechanism through the process of biochemical and structural changes in the TDP-43 molecule in neurons and/or glial cells may be related to the neurodegeneration in ALS, FTLD-U and G-PDC. The deposition of TDP-43 in brains of G-ALS patients should be analysed as well. It might also be important to investigate the relationship between environmental or genetic factors and dysfunction or deposition of TDP-43 in these disorders.

Acknowledgements

This work was supported by a Grant-in-Aid for Scientific Research on Priority Areas—Research on Pathomechanisms of Brain Disorders (to M.H.) and a Grant-in-Aid for Scientific Research (B) (to M.H.), both from the Ministry of Education, Culture, Sports, Science and Technology of Japan.

References

Arai T, Hasegawa M, Akiyama H, Ikeda K, Nonaka T, Mori H, et al. TDP-43 is a component of ubiquitin-positive tau-negative inclusions in frontotemporal lobar degeneration and amyotrophic lateral sclerosis. Biochem Biophys Res Commun 2006; 351: 602–11.

Ayala Y, Pantano S, D'Ambrogio A, Buratti E, Brindisi A, Marchetti C, et al. Human, drosophila, and C. elegans TDP43: nucleic acid binding properties and splicing regulatory function. J Mol Biol 2005; 348: 575–88.

Baker M, Mackenzie IR, Pickering-Brown SM, Gass J, Rademakers R, Lindholm C, et al. Mutations in progranulin cause tau-negative frontotemporal dementia linked to chromosome 17. Nature 2006; 442: 916–9.

Bergmann M, Kuchelmeister K, Schmid KW, Kretzschmar HA, Schröder R. Different variants of frontotemporal dementia: a neuropathological and immunohistochemical study. Acta Neuropathol (Berl) 1996; 92: 170–9.

Boeve BF, Baker M, Dickson DW, Parisi JE, Giannini C, Josephs KA, et al. Frontotemporal dementia and parkinsonism associated with the IVS1 + 1G→A mutation in progranulin: a clinicopathological study. Brain 2006; 129: 3103–14.

Buratti E, Brindisi A, Giombi M, Tisminetzky S, Ayala YM, Baralle FE. TDP-43 binds heterogeneous nuclear ribonucleoprotein A/B through its C-terminal tail. J Biol Chem 2005; 280: 37572–84.

Buratti E, Dork T, Zuccato E, Pagani F, Romano M, Baralle FE. Nuclear factor TDP-43 and SR proteins promote in vitro and in vivo CFTR exon 9 skipping. EMBO J 2001; 20: 1774–84.

Cavanagh JB. Corpora-amylacea and the family of polyglucosan diseases. Brain Res Rev 1999; 29: 265–95.

Cox PA, Banack SA, Murch SJ. Biomagnification of cyanobacterial neurotoxins and neurodegenerative disease among the Chamorro people of Guam. Proc Natl Acad Sci USA 2003; 100: 13380–3.

Cruts M, Gijselinck I, van der Zee J, Engelborghs S, Wils H, Pirici D, et al. Null mutations in progranulin cause ubiquitin-positive frontotemporal dementia linked to chromosome 17q21. Nature 2006; 442: 920–4.

Davidson Y, Kelley T, Mackenzie IRA, Pickering-Brown S, Du Plessis D, Neary D, et al. Ubiquitinated pathological lesions in frontotemporal lobar degeneration contain the TAR DNA-binding protein, TDP-43. Acta Neuropathol (Berl) 2007; doi: 10.1007/s00401-006-0189-y.

Forman MS, Mackenzie IR, Cairns NJ, Swanson E, Boyer PJ, Drachman DA, et al. Novel ubiquitin neuropathology in frontotemporal dementia with valosin-containing protein gene mutations. J Neuropathol Exp Neurol 2006; 65: 571–81.

Gass J, Cannon A, Mackenzie IR, Boeve B, Baker M, Adamson J, et al. Mutations in progranulin are a major cause of ubiquitin-positive frontotemporal lobar degeneration. Hum Mol Genet 2006; 15: 2988–3001.

Gentleman SM, Perl D, Allsop D, Clinton J, Royston MC, Roberts GW. Beta (A4)-amyloid protein and parkinsonian dementia complex of Guam. Lancet 1991; 337: 55–6.

Guyant-Marechal L, Laquerriere A, Duyckaerts C, Dumanchin C, Bou J, Dugny F, et al. Valosin-containing protein gene mutations. Clinical and neuropathological features. Neurology 2006; 67: 644–51.

Hermosura MC, Nayakanti H, Dorovkov MV, Calderon FR, Ryazanov AG, Haymer DS, et al. A TRPM7 variant shows altered sensitivity to magnesium that may contribute to the pathogenesis of two Guamanian neurodegenerative disorders. Proc Natl Acad Sci USA 2005; 102: 11510–5.

Hirano A, Kurland LT, Krooth RS, Lessell S. Parkinsonism-dementia complex, an endemic disease on the island of Guam. I. Clinical features. Brain 1961; 84: 642–61.

Hirano A, Malamud N, Elizan TS, Krurland LT. Amyotrophic lateral sclerosis and Parkinsonism-dementia complex on Guam. Further pathologic studies. Arch Neurol 1966; 15: 35–51.

Hof PR, Perl DP, Loerzel AJ, Morrison JH. Neurofibrillary tangle distribution in the cerebral cortex of parkinsonism-dementia cases from Guam: differences with Alzheimer's disease. Brain Res 1991; 564: 306–13.

Huey ED, Grafman J, Wassermann EW, Pietrini P, Tierney MC, Ghetti B, et al. Characteristics of frontotemporal dementia patients with a progranulin mutation. Ann Neurol 2006; 60: 374–80.

Ikemoto A, Hirano A, Akiguchi I, Kimura J. Comparative study of ubiquitin immunoreactivity of hippocampal granular cells in amyotrophic lateral sclerosis with dementia, Guamanian amyotrophic lateral sclerosis and Guamanian parkinsonism-dementia complex. Acta Neuropathol (Berl) 1997; 93: 265–70.

Iseki E, Li F, Odawara T, Hino H, Suzuki K, Kosaka K, et al. Ubiquitin-immunohistochemical investigation of atypical Pick's disease without Pick bodies. J Neurol Sci 1998; 159: 194–201.

Jackson M, Lennox G, Lowe J. Motor neuron disease-inclusion dementia. Neurodegeneration 1996; 5: 339–50.

Mackenzie IRA, Baborie A, Pickering-Brown S, Du Plessis D, Jaros E, Perry RH, et al. Heterogeneity of ubiquitin pathology in frontotemporal lobar degeneration: classification and relation to clinical phenotype. Acta Neuropathol (Berl) 2006*a*; 112: 539–49.

Mackenzie IRA, Baker M, Pickering-Brown S, Hsiung GYR, Lindholm C, Dwosh E, et al. The neuropathology of frontotemporal lobar degeneration caused by mutations in the progranulin gene. Brain 2006*b*; 129: 3081–90.

Mackenzie IRA, Feldman H. Neuronal intranuclear inclusions distinguish familial FTD-MND type from sporadic cases. Acta Neuropathol (Berl) 2003; 105: 543–8.

Mackenzie IRA, Feldman HH. Ubiquitin immunohistochemistry suggests classic motor neuron disease, motor neuron disease with dementia, and frontotemporal dementia of the motor neuron disease type represent a clinicopathological spectrum. J Neuropathol Exp Neurol 2005; 64: 730–9.

Masellis M, Momeni P, Meschino W, Heffner R Jr, Elder J, Sato C, et al. Novel splicing mutation in the progranulin gene causing familial corticobasal syndrome. Brain 2006; 129: 3115–23.

Mori H, Kondo J, Ihara Y. Ubiquitin is a component of paired helical filaments in Alzheimer's disease. Science 1987; 235: 1641–4.

Mukherjee O, Pastor P, Cairns NJ, Chakraverty S, Kauwe JSK, Shears S, et al. HDDD2 is a familial frontotemporal lobar degeneration with ubiquitin-positive tau-negative inclusions caused by a missense mutation in the signal peptide of progranulin. Ann Neurol 2006; 60: 314–22.

Nakano I, Hirano A. Neuron loss in the nucleus basalis of Meynert in parkinsonism-dementia complex of Guam. Ann Neurol 1983; 13: 87–91.

Neumann M, Mackenzie IR, Cairns NJ, Boyer PJ, Markesbery WR, Smith CD, et al. TDP-43 in the ubiquitin pathology of frontotemporal dementia with VCP gene mutations. J Neuropathol Exp Neurol 2007; 66: 152–7.

Neumann M, Sampathu DM, Kwong LK, Truax AC, Micsenyi MC, Chou TT, et al. Ubiquitinated TDP-43 in frontotemporal lobar degeneration and amyotrophic lateral sclerosis. Science 2006; 314: 130–3.

Okamoto K, Hirai S, Yamazaki T, Sun X, Nakazato Y. New ubiquitin-positive intraneuronal inclusions in the extra-motor cortices in patients with amyotrophic lateral sclerosis. Neurosci Lett 1991; 129: 233–6.

Okamoto K, Murakami N, Kusada H, Yoshida M, Hashizume Y, Nakazato Y, et al. Ubiquitin-positive intraneuronal inclusions in the extramotor cortices of presenile dementia patients with motor neuron disease. J Neurol 1992; 239: 426–30.

Ou SH, Wu F, Harrich D, Garcia-Martinez LF, Gaynor RB. Cloning and characterization of a novel cellular protein, TDP-43, that binds to human immunodeficiency virus type 1 TAR DNA sequence motifs. J Virol 1995; 69: 3584–96.

Oyanagi K, Kawakami E, Kikuchi-Horie K, Ohara K, Ogata K, Takahama S, et al. Magnesium deficiency over generations in rats with special references to the pathogenesis of the Parkinsonism-dementia complex and amyotrophic lateral sclerosis of Guam. Neuropathology 2006; 26: 115–28.

Oyanagi K, Makifuchi T, Ohtoh T, Chen KM, Gajdusek DC, Chase TN. Distinct pathological features of the gallyas- and tau-positive glia in the Parkinsonism-dementia complex and amyotrophic lateral sclerosis of Guam. J Neuropathol Exp Neurol 1997; 56: 308–16.

Oyanagi K, Makifuchi T, Ohtoh T, Chen KM, van der Schaaf T, Gajdusek DC, et al. Amyotrophic lateral sclerosis of Guam: the nature of the neuropathological findings. Acta Neuropathol (Berl) 1994*a*; 88: 405–12.

Oyanagi K, Makifuchi T, Ohtoh T, Ikuta F, Chen KM, Chase TN, et al. Topographic investigation of brain atrophy in parkinsonism-dementia complex of Guam: a comparison with Alzheimer's disease and progressive supranuclear palsy. Neurodegeneration 1994*b*; 3: 301–4.

Oyanagi K, Wada M. Neuropathology of parkinsonism-dementia complex and amyotrophic lateral sclerosis of Guam: an update. J Neurol 1999; 246 ((Suppl 2:II): 19–27.

Pickering-Brown SM, Baker M, Gass J, Boeve BF, Loy CT, Brooks WS, et al. Mutations in progranulin explain atypical phenotypes with variants in MAPT. Brain 2006; 129: 3124–6.

Schmidt ML, Lee VMY, Saido T, Perl D, Schuck T, Iwatsubo T, et al. Amyloid plaques in Guam amyotrophic lateral sclerosis/parkinsonism-dementia complex contain species of A beta similar to those found in the amyloid plaques of Alzheimer's disease and pathological aging. Acta Neuropathol (Berl) 1998; 96: 487–94.

Sebeo J, Hof PR, Perl DP. Occurrence of α-synuclein pathology in the cerebellum of Guamanian patients with parkinsonism-dementia complex. Acta Neuropathol (Berl) 2004; 107: 497–503.

Snowden JS, Pickering-Brown SM, Mackenzie IR, Richardson AMT, Varma A, Neary D, et al. Progranulin gene mutations associated with frontotemporal dementia and progressive non-fluent aphasia. Brain 2006; 129: 3115–23.

Wang I-F, Reddy NM, Shen C-KJ. Higher order arrangement of the eukaryotic nuclear bodies. Proc Natl Acad Sci USA 2002; 99: 13583–8.

Wightman G, Anderson VER, Martin AJ, Swash M, Anderson BH, Neary D, et al. Hippocampal and neocortical ubiquitin-immunoreactive inclusions in amyotrophic lateral sclerosis with dementia. Neurosci Lett 1992; 139: 269–74.

Woulfe J, Kertesz A, Munoz DG. Frontotemporal dementia with ubiquitinated cytoplasmic and intranuclear inclusions. Acta Neuropathol (Berl) 2001; 102: 94–102.

Yamazaki M, Hasegawa M, Mori O, Murayama S, Tsuchiya K, Ikeda K, et al. Tau-positive fine granules in the cerebral white matter: a novel finding among the tauopathies exclusive to parkinsonism-dementia complex of Guam. J Neuropathol Exp Neurol 2005; 64: 839–46.

Human Molecular Genetics, 2007, Vol. 16, No. 3 **295–306**
doi:10.1093/hmg/ddl463
Advance Access published on December 21, 2006

Two sites in the *MAPT* region confer genetic risk for Guam ALS/PDC and dementia

Purnima Desai Sundar[1,5], Chang-En Yu[1,5], Weiva Sieh[2], Ellen Steinbart[1,5], Ralph M. Garruto[6], Kiyomitsu Oyanagi[7], Ulla-Katrina Craig[8], Thomas D. Bird[4,5], Ellen M. Wijsman[2,3], Douglas R. Galasko[9] and Gerard D. Schellenberg[1,4,5,*]

[1]Department of Medicine, Division of Gerontology and Geriatric Medicine, [2]Department of Medicine, Division of Medical Genetics, [3]Department of Biostatistics and [4]Department of Neurology and Pharmacology, University of Washington, Seattle, WA 98195, USA, [5]Geriatric Research Education and Clinical Center, Veterans Affairs Puget Sound Health Care System, Seattle Division, Seattle, WA 98108, USA, [6]Department of Anthropology, Laboratory of Biomedical Anthropology and Neurosciences, Binghamton University, SUNY-Binghamton, NY 13902-6000, USA, [7]Department of Neuropathology, Tokyo Metropolitan Institute for Neuroscience, Tokyo, Japan, [8]University of Guam, Mangilao, Guam 96923, USA and [9]Department of Neurosciences, University of California, San Diego, La Jolla CA 92093-0662, USA

Received October 7, 2006; Revised and Accepted December 6, 2006

Unusual forms of amyotrophic lateral sclerosis (ALS-G), Parkinsonism dementia complex (PDC-G) and Guam dementia (GD) are found in Chamorros, the indigenous people of Guam. Neurofibrillary tangles composed of hyperphosphorylated tau are a neuropathologic feature of these closely related disorders. To determine if variation in the gene that encodes microtubule-associated protein tau gene (*MAPT*) contributes to risk for these disorders, we genotyped nine single nucleotide polymorphism (SNP) sites and one insertion/deletion in the 5′ end of *MAPT* in 54 ALS-G, 135 PDC-G, 153 GD and 258 control subjects, all of whom are Chamorros. Variation at three SNPs (sites 2, 6 and 9) influenced risk for ALS-G, PDC-G and GD. SNP2 acts through a dominant mechanism and is independent of the risk conferred by SNPs 6 and 9, the latter two acting by a recessive mechanism. Persons with the high-risk SNP6 and SNP9 AC/AC diplotype had an increased risk of 3-fold [95% confidence interval (CI) = 1.10–8.25] for GD, 4-fold (95% CI = 1.40–11.64) for PDC-G and 6-fold (95% CI = 1.44–32.14) for ALS-G, compared to persons with other diplotypes after adjusting for SNP2. Carriers of the SNP2 G allele had an increased risk of 1.6-fold (95% CI = 1.00–2.62) for GD, 2-fold (95% CI = 1.28–3.66) for PDC-G, and 1.5-fold (95% CI = 0.74–3.00) for ALS-G, compared to non-carriers after adjusting for SNPs 6 and 9. Others have shown that SNP6 is also associated with risk for progressive supranuclear palsy. These two independent *cis*-acting sites presumably influence risk for Guam neurodegenerative disorders by regulating *MAPT* expression.

INTRODUCTION

In the 1950s, amyotrophic lateral sclerosis (ALS) was highly prevalent (143 per 100 000) in Chamorros, the indigenous people of Guam (1). ALS in Guam (ALS-G) is clinically similar to ALS in other populations (1,2). However, unlike typical ALS, where neurodegeneration is confined to spinal cord motor neurons, in ALS-G, central nervous system changes occur including numerous neurofibrillary tangles (NFTs) typically in the neocortex, hippocampus and subcortical regions (2–6). A related disorder, parkinsonism dementia complex (PDC), is also highly prevalent in the same Chamorro population (2,7). The clinical symptoms of PDC in Guam (PDC-G) are parkinsonism (with bradykinesia, gait impairment, rigidity and often resting tremor), accompanied by progressive dementia. The neuropathologic features of PDC-G overlap with ALS-G (4,5,8,9) with a higher NFT burden in brain regions corresponding to the respective clinical

*To whom correspondence should be addressed at: GRECC S-182B, Veterans Affairs Puget Sound Health Care System, 1660 S. Columbian Way, Seattle, WA 98108, USA. Tel: +1 2067642701; Fax: +1 2067642569; Email: zachdad@u.washington.edu.

phenotypes of the two disorders. Spinal cord NFTs are found in both ALS-G and PDC-G (10,11). More recently, late-life dementia without parkinsonism in Chamorros, referred to here as Guam dementia (GD), has been studied (12). The relationships between GD and ALS-G, and PDC-G and Alzheimer's disease (AD) are unclear. Preliminary neuropathology studies suggest that GD has prominent AD-type tangles with less prominent amyloid or neuritic pathology than that found in typical AD (13).

The etiology of ALS-G, PDC-G and GD, collectively referred to here as Guam neurodegenerative disorders, is unknown, though there is substantial evidence supporting a genetic hypothesis. Early work noted highly variable prevalence rates in different Guam villages. Families with multiple cases of ALS-G and PDC-G were common, numerous multigenerational pedigrees with multiple cases of ALS-G, PDC-G or both were described, and the affected father–son pairs were documented (7,14–18). In several studies, 35–40% of probands have relatives with ALS-G/PDC-G (14,17). In the village of Umatac, which had the highest prevalence of the disease (250/100 000) (1), segregation analysis suggested a major gene with penetrance possibly affected by an environmental factor(s) (19). More recently, Plato *et al.* (20), who followed the relatives of a cohort of ALS-G/PDC-G cases and controls for over 40 years, found more new cases in the offspring of affected subjects compared to relatives of controls. Another cluster of ALS and PDC exists on the Kii peninsula of Japan, where the disease is strongly familial (21–25). An environmental hypothesis is also plausible, supported by the decline in incidence of ALS-G over the past 40 years and an increase in onset ages for both ALS-G and PDC-G (2,12,26). No specific environmental factor has been identified though several have been proposed including β-methylamino-alanine (BMAA), a neurotoxin found in cycad seeds (27). The most parsimonious hypothesis is that there are both genetic and environmental components to Guam neurodegenerative disorders.

Identification of the genes that influence susceptibility to Guam neurodegenerative disorders is important to understanding the etiology of these disorders. ALS-G, PDC-G and GD are tauopathies, a class of diseases where aggregated tau (e.g. NFTs) is a prominent neuropathologic feature. For some tauopathies, genetic variation in *MAPT*, the gene that encodes for tau, causes or contributes to the disease. Mutations in *MAPT* cause frontotemporal dementia (FTD) with parkinsonism—chromosome 17 type (FTDP-17) (28–30), an autosomal dominant group of tauopathies with variable phenotypes. However, no *MAPT* mutations have been identified in subjects with Guam disorders (31,32) and the major locus responsible for this disease remains to be found (33). More subtle genetic changes in *MAPT*, presumably in regulatory regions, increase susceptibility to progressive supranuclear palsy (PSP) (34–36), FTD (37–39), corticobasal degeneration (CBD) (40,41) and possibly AD (42), all of which are tauopathies. Although the polymorphic site responsible for elevated risk has been difficult to identify definitively, recent work suggests that alleles at a single nucleotide polymorphism (SNP) in the first intron of tau (intron 0) influence *MAPT* expression and may be the causative site (43). We previously examined 49 ALS-G cases, 82 PDC-G cases and 78 Chamorro controls and reported significant association with the dinucleotide repeat marker CA3662, located 23.9 kb upstream of the transcription start site of *MAPT* (32) (Fig. 1). Since the CA3662 association is likely due to linkage disequilibrium (LD) with the causative variant in the surrounding region, and because recent work on the association between *MAPT* genotypes and PSP implicated SNPs in the 5′ end of *MAPT* (35,43,44), we examined SNPs in corticotrophin-releasing hormone receptor 1 (*CRHR1*) and intramembrane protease 5 (*IMP5*), genes that are upstream of *MAPT*, and SNPs within the 5′ end of *MAPT* (Fig. 1) in a larger case–control dataset of 54 ALS-G, 135 PDC-G, 153 GD and 258 Chamorro controls. We identified two independent regions that contribute to Guam neurodegenerative disorder risk. One is in the *IMP5* region upstream of *MAPT* and acts in a dominant mechanism. The second is in *MAPT*, acts by a recessive mechanism, and possibly corresponds to the same site(s) in *MAPT* that confer risk for PSP.

RESULTS

In the previous work, we showed an allelic association between ALS-G, PDC-G and an allele of a polymorphic site that is 23.9 kb from the 5′ end of *MAPT* (32). Other work showed that for PSP, a tauopathy with some overlapping features with ALS-G and PDC-G, SNP sites within *MAPT* are associated with disease risk (35,43). To determine which polymorphic site(s) in the *MAPT* region contributes to risk of ALS-G and PDC-G, we genotyped eight markers within *MAPT* between the promoter and intron 9, and two in the flanking region 5′ of *MAPT* (Table 1, Fig. 1). Also, we examined the same loci in a GD population to determine if the same alleles confer risk to this related disorder. The cases and controls used were Chamorros ascertained in Guam. Controls were 258 Chamorro subjects with mean age 66.5 ± 14.0 years (35% male) who were cognitively normal, and did not have other neurologic disorders. The case groups were 54 ALS-G subjects (mean age at onset 51.1 ± 11.6 years; 65% male), 135 PDC-G subjects (mean age at onset 64.2 ± 10.1 years; 53% male) and 153 GD cases (mean age at onset 74.9 ± 7.2 years; 27% male).

Allele frequencies for the markers genotyped are given in Table 2. We used marker del-in9 to tag the H1/H2 haplotype system, an inversion polymorphism where approximately 900 kb of chromosome 17 spanning *MAPT* are in opposite orientations in the two haplotypes (45). All SNPs genotyped in this study are within the chromosome 17 segment inverted in this polymorphism. The H1 haplotype is associated with increased risk for PSP and is more common than the H2 haplotype. In our Chamorro samples, the frequency of the H1 haplotype ranged from 95.9% in the PDC-G group to 91.3% in controls (Table 2), which is higher than in typical Caucasian controls (74–80%) (42,45,46). Consistent with previous reports in Caucasians, the H2 haplotype in Chamorros was much less diverse than the H1 haplotype (43,45); nearly all of the SNPs we examined were monomorphic in our sample of H2 haplotypes and we observed strong pairwise LD between the H1/H2 inversion polymorphism and *MAPT* region SNPs in Chamorro subjects. $|D'|$ for the H1/H2

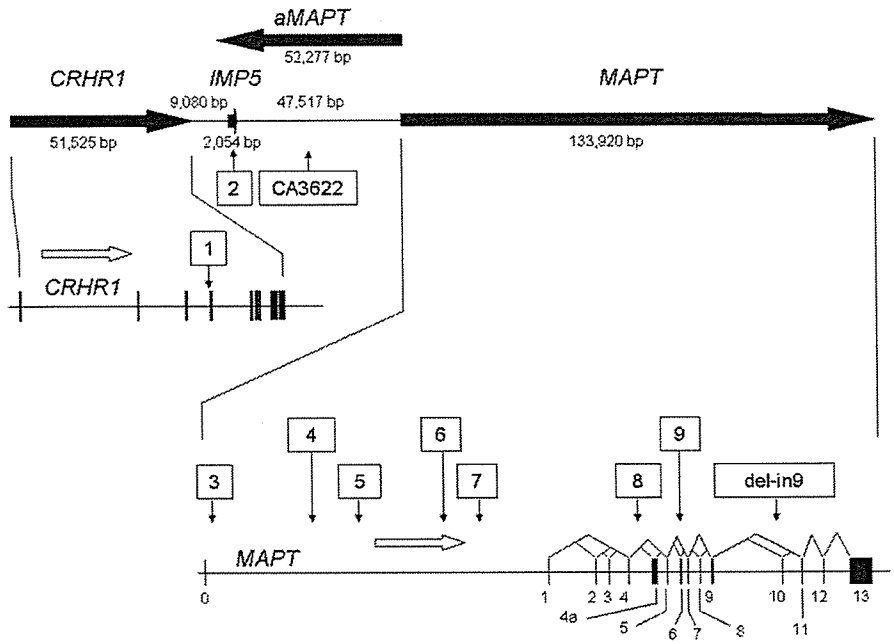

Figure 1. The chromosome 17 *MAPT* region. The distances shown are proportional to the actual sizes of the different genomic elements. Numbers in boxes refer to the SNPs used in this study. The direction of transcription is indicated by the direction of the arrows used to represent *CRHR1*, *IMP5*, *aMAPT* and *MAPT*. Alternatively spliced *MAPT* exons (solid boxes) are indicated by connecting lines above each exon.

inversion polymorphism and nine *MAPT* SNPs, respectively, was 1.0 for SNPs 2 and 3; >0.8 for SNPs 1, 4–6 and 9; and >0.6 for SNPs 6 and 7.

We restricted all subsequent analyses to individuals who are homozygous for the H1 lineage, for two reasons. First, the Chamorro people of Guam have a much higher incidence of ALS than Caucasians and PDC-G does not have a clinicopathological equivalent in Caucasians. Since Chamorros and Caucasians also have a different H1 frequency, a disease association involving SNPs that are associated with the inversion polymorphism could reflect the confounding effect of population admixture rather than a true disease association. Second, since inversions result in suppression of recombination, the H1 and H2 lineages represent evolutionarily and reproductively isolated regions of the genome even within a panmictic population. Therefore, analysis of just one of these lineages is necessary to permit evaluation of individual SNP effects separately from effects attributable to the inversion polymorphism. LD patterns among the nine *MAPT* region SNPs in 214 H1/H1 controls are shown in Table 3. LD was strongest ($|D'| \geq 0.8$ and/or $r^2 \geq 0.4$) between SNPs 1–2, 3–5, 6–7 and 8–9, and was relatively weak between the other SNPs.

Global differences in allele frequencies for SNPs 2 ($P = 0.007$), 6 ($P = 0.011$), 7 ($P = 0.055$) and 9 ($P = 0.032$) were observed among H1 homozygotes in the ALS-G, PDC-G, GD and control groups (Table 2). Allele frequencies did not differ significantly among the three case groups. Compared to controls, cases tended to have higher frequencies of the minor 'A' allele at SNP2, major 'A' allele at SNP6, major 'A' allele at SNP7 and major 'C' allele at SNP9. There was no evidence of Hardy–Weinberg disequilibrium (HWD) at any of the nine SNPs in H1/H1 controls or cases with PDC-G or GD. However, Hardy–Weinberg equilibrium in the 49 H1/H1 ALS-G cases was rejected at SNPs 3 ($P = 0.004$), 4 ($P = 0.010$) and 5 ($P = 0.023$). Whereas allelic association tests are susceptible to false-positive results as a consequence of HWD, genotypic association tests remain valid (47). Global genotypic (Table 4) and allelic (Table 2) association screening tests yielded comparable results for SNPs 2, 6, 7 and 9. Exploratory analyses were also conducted for SNPs 3 and 5 based on the global genotype association test results, and possible univariate associations with ALS-G or PDC-G (data not shown, Supplementary Material, Table S1).

Univariate logistic regression analyses showed that the risk of GD and PDC-G in Guam was significantly associated with SNPs 2, 6, 7 and 9 (Table 4). Evidence for association was also found for SNP3 and ALS-G (data not shown, Supplementary Material, Table S1), although the number of ALS-G cases was relatively small. The G allele of SNP2 in *IMP5* conferred increased risk in a dominant manner, whereas the SNP5–7 A and SNP3 and 9 C alleles appear to confer risk in a recessive manner (Table 4, data not shown, Supplementary Material, Table S1). *MAPT* region SNPs were fit as either dominant or recessive genetic effects in higher order models for the sake of model parsimony. No significant evidence of an association was found between Apolipoprotein E (*APOE*) and ALS-G, PDC-G or GD in Guam (Table 2).

A fortuitous aspect of the data allowed us to infer that the associations observed for SNPs 6 and 7 could largely be explained by SNP6. All 181 H1/H1 individuals with the

Table 1. Polymorphic sites

SNP/ polymorphism	dbSNP number	Gene	Sequence location (bp)	Alleles	Distance to next SNP	Assay type	PCR primers or TaqMan assay number	Restriction enzyme or reporter sequence
1	rs242937	*CRHR1* (intron 3)	41,254,149	A,G	24,811	RFLP	F-GCTCTACCACAAG AAGCCCTGTC R-CTGGGCTGTTCC TTTGCAAGT	MnlI
2	rs242944	*IMP5* (exon 1)	41,278,960	A,G	49,751	TaqMan	C_2257672_10	
3	rs3744457	*MAPT* (intron 0)	41,328,711	C,T	20,493	RFLP	F-CACTTTAGTTGCC CTTCCCCCT R-CTCCGAGCGCTG AGAAAGAAAT	NlaIII
4	rs3785880	*MAPT* (intron 0)	41,349,204	T,G	9,256	TaqMan	F-GGCACTGCTGGT TTGAAAGG R-TGGGCAGGGTG TGAATCC	[VIC] CCACGG**C** AGTTACT [FAM] CCACGG **A**AGTTACT
5	rs2055797	*MAPT* (intron 0)	41,358,460	A,T	17,113	TaqMan	F-CAAACCGTCTTG CACAGTGT R-GGCTGCAGTGG TTTCTTCAG	[VIC] CCCTCTC C**T**GGGTTT [FAM] CCTCTCC **A**GGGTTT
6	rs242557	*MAPT* (intron 0)	41,375,573	A,G	7,226	TaqMan	F-CGTTTCTTCTTCC TTACAAAGCAGTT R-CCCTGGTCCCGT GACA	[VIC] CCCAGGG T**A**CACCAG [FAM] CCAGGGT **G**CACCAG
7	rs242562	*MAPT* (intron 0)	41,382,599	A,G	32,166	TaqMan	C_3202957_10	
8	rs2435207	*MAPT* (intron 4)	41,414,765	A,G	8,454	TaqMan	F-CGTGCAGAGCCC TTCCT R-AGAAGCCCCATTC AGATCTATCCA	[VIC] CTTGTCTG TG**A**TCAGTG [FAM] CTTGTCT GTG**G**TCAGTG
9	rs2258689	*MAPT* (exon 6)	41,423,219	C,T	18	TaqMan	F-GTGCCCAGAGCC ACCTT R-CTGCCAGTTCGG GAAGTGA	[VIC] CAGAAGA GACGT**G**TTTAG [FAM]CAGAAGA GACGT**A**TTTAG
del-in9		*MAPT* (intron 9)	41,442,488	H1,H2	19,297	fragment size	F-GGAAGACGTTCTCACT GATCTG R-AGGAGTCTGGCTTCAG TCTCTC	

The sequence location is from NCBI Build 36.1. Nucleotides in boldface are alleles of SNPs.

Table 2. Allele frequencies by C17 inversion status and diagnosis group

SNP	Alleles (major/minor)	All H1 and H2 genotypes				H1/H1 homozygotes only				
		Controls ($n = 258$)[a]	GD ($n = 153$)	PDC-G ($n = 135$)	ALS-G ($n = 54$)	Controls ($n = 214$)	GD ($n = 136$)	PDC-G ($n = 124$)	ALS-G ($n = 49$)	P^*
Markers 5′ to *MAPT*										
1[b]	G/A	24.7	24.5	26.5	17.6	17.7	19.6	23.2	13.3	0.149
2[c]	A/G	40.6	46.1	50.4	42.6	34.4	42.3	47.6	40.8	0.007
MAPT markers										
3[d]	C/T	50.0	47.1	40.7	44.4	44.9	44.5	39.0	40.8	0.453
4[e]	T/G	33.3	34.3	28.7	33.3	36.3	37.1	30.9	34.7	0.445
5	A/T	48.6	42.2	37.8	44.4	43.9	39.0	35.9	40.8	0.210
6	A/G	51.4	40.5	39.3	45.4	47.4	36.8	36.7	40.8	0.011
7[f]	A/G	44.9	36.3	34.4	40.7	40.6	32.4	31.4	36.7	0.055
8	G/A	16.1	12.1	13.7	16.7	17.1	12.9	14.9	17.4	0.458
9[g]	C/T	50.2	39.2	39.9	41.7	45.5	35.3	37.3	37.8	0.032
del-in9	H1/H2	8.7	5.9	4.1	4.6					
APOE	ε2	4.5	4.0	6.7	1.9	4.9	4.2	6.1	2.0	0.523
	ε3	90.5	91.2	90.3	90.7	90.2	91.7	90.7	90.8	
	ε4	5.0	4.7	3.0	7.4	4.9	4.2	3.2	7.1	

Minor allele frequency for diallelic variants; all allele frequencies for *APOE*, a triallelic variant system.
*Fisher's exact test of global allele frequency differences among H1 homozygotes in the four diagnosis groups.
[a]*n*, total number of individuals; 2*n*, total number of alleles.
[b]Two H1/H1 controls, one H2/H2 control, six H1/H1 GD cases and one H1/H1 PDC case had missing genotypes at this site.
[c]Two H1/H1 controls had missing genotypes at this site.
[d]One H1/H1 PDC case had a missing genotype at this site.
[e]Three H1/H1 controls, one H1/H2 control and one H1/H1 PDC case had missing genotypes at this site.
[f]Two H1/H1 controls had missing genotypes at this site.
[g]One H1/H1 control and two H1/H1 PDC cases had missing genotypes at this site.

high-risk A/A genotype at SNP6 also had the high-risk A/A genotype at SNP7 with the exception of two PDC-G cases, who had the low-risk G/A genotype at SNP7. The SNP6 A allele was therefore a nearly perfect marker for the AA haplotype at SNPs 6 and 7 in this population. In contrast, 39/218 (17.9%) H1/H1 individuals with the high-risk A/A genotype at SNP7 had the low-risk G/A or G/G genotypes at SNP6. If the homozygous AA diplotype at SNPs 6 and 7 were truly responsible for disease, then using the SNP7 rather than SNP6 A/A genotype as a marker would lead to an attenuated estimate of the genetic effect because of the noise introduced by including 39 individuals with the low-risk GA/AA or GA/GA diplotypes at SNPs 6 and 7 into the 'exposed' category. Furthermore, including both SNPs 6 and 7 in the model would reduce the statistical significance of either effect because they are measures of the same underlying haplotype. The magnitude of the estimated risks of GD, PDC-G or ALS-G associated with SNP6 were stronger than SNP7 in both univariate (Table 4) and higher order models, and neither SNP was statistically significant when both were included in the model. These results indicated that the homozygous AA diplotype at SNPs 6 and 7, almost perfectly captured by the SNP6 A/A genotype, was associated with disease risk.

Combinations of two or more *MAPT* SNPs were analyzed to identify independent risk factors and interactions between genetic variants. Possession of the 'G' allele at SNP2 was an independent risk factor for both GD and PDC-G as well as for all cases combined (Table 5). Additionally, a significant interaction between the high-risk A/A and C/C genotypes at SNPs 6 and 9 was found for all three case groups and the combined set of cases. No significant three-way interaction was found, and *APOE* did not confound or weaken the *MAPT* effects.

The final genetic model for GD and PDC-G included SNP2 and the main effects and interaction of SNPs 6 and 9 (Table 5). When the final genetic model for GD and PDC-G was fit for ALS-G, a similar risk pattern emerged (Table 5). H1/H1 persons with the homozygous AC diplotype at SNPs 6 and 9 had a 3-fold [95% confidence interval (CI) = 1.10–8.25] increased risk of GD, 4-fold (95% CI = 1.40–11.64) increased risk of PDC-G and 6-fold (95% CI = 1.44–32.14) increased risk of ALS-G, compared to persons who were not homozygous for this diplotype after adjusting for SNP2. H1/H1 carriers of the SNP2 G allele had a 1.6-fold (95% CI = 1.00–2.62) increased risk of GD, 2-fold (95% CI = 1.28–3.66) increased risk of PDC-G and 1.5-fold (95% CI = 0.74–3.00) increased risk of ALS compared to non-carriers after adjusting for SNPs 6 and 9. In an analysis of all cases combined, the risk of developing GD, PDC-G or ALS-G was independently increased by 1.7-fold (95% CI = 1.18–2.60) in carriers of the SNP2 G allele, and 3.8-fold (95% CI = 1.64–8.78) in persons with the homozygous AC diplotype at SNPs 6 and 9.

The high-risk AC diplotype, or haplotype, defined by SNPs 6 and 9 is unlikely to represent the H1c haplotype reported to be associated with PSP and CBD (36). The frequency of H1 haplotypes containing this AC haplotype was significantly higher in the case samples (0.484–0.525) than in the control samples (0.355), as was the 3-SNP haplotype, TAC, that also includes SNP4 (frequency 0.415–0.437 in the case samples versus 0.296 in the control samples) (Supplementary Material, Table S3). Although the A allele of SNP6 is the

Table 3. Pairwise LD among SNPs in Guam H1/H1 controls

		r^2-value								
		1[a]	2	3	4	5	6	7	8	9
$\|D'\|$	1[a]	–	0.40	0.00	0.00	0.00	0.03	0.02	0.01	0.08
	2	1.00	–	0.09	0.04	0.12	0.17	0.11	0.00	0.00
	3	0.08	0.47	–	0.66	0.70	0.21	0.13	0.03	0.02
	4	0.08	0.35	0.98	–	0.47	0.10	0.22	0.05	0.00
	5	0.07	0.53	0.85	0.80	–	0.34	0.22	0.02	0.02
	6	0.38	0.61	0.48	0.40	0.62	–	0.58	0.01	0.04
	7	0.34	0.56	0.39	0.52	0.50	0.87	–	0.02	0.01
	8	0.09	0.14	0.36	0.36	0.24	0.15	0.25	–	0.25
	9	0.54	0.04	0.14	0.04	0.13	0.22	0.09	1.00	–

[a]Numbers in the left most column and the top row refer to the polymorphism site numbers in Table 1.

allele on the H1c haplotype, estimation of 5-SNP haplotypes (including the three SNPs used to tag H1c) in the JPT HapMap sample shows that the frequency of the H1c haplotype is only 2.4% (Supplementary Material, Table S4). Also, the C allele of SNP9 perfectly predicts the existence of allele C for SNP rs2471738. Since the H1c haplotype has allele T for rs2471738, based on the JPT 5-SNP haplotype frequencies, the conditional probability that the SNP6–9 AC haplotype (or the SNP4–6–9 TAC haplotype) represents that the H1c haplotype is 0.

DISCUSSION

The results described above show that genetic variation in the *MAPT* region contributes to risk for ALS-G, PDC-G and GD. Our previous work (32) showed an association between a single polymorphism (CA3662, Fig. 1) and ALS-G and PDC-G. Here, we confirm and extend our original findings by showing risk associated with additional SNPs in a larger sample. Also, these results extend our findings to GD, which was not previously studied. An intriguing novel finding is that the risk for Guam neurologic disorders is independently determined by SNPs in two different locations, one within *MAPT* and another upstream of *MAPT* in or near *IMP5*.

Genotypes within *MAPT* contribute to susceptibility to Guam neurologic disorders by a recessive mechanism. For SNPs 6, 7 and 9, homozygous genotypes (A/A, A/A and C/C, respectively) confer risk, whereas the other 2 genotypes for each site do not (Table 4). In studies of PSP, SNP6 genotypes also show a statistically significant association with risk (43,44), and in both our study and the work on PSP, the A allele is the high-risk allele. SNP6, located in the first intron of *MAPT* (Fig. 1), is in a region conserved across a number of mammalian species (43,48) suggesting a functional role in *MAPT* regulation. Rademaker *et al.* (43) showed that the 182 bp region containing SNP6 can act as a *cis*-acting transcriptional enhancer in a cell culture model and that the enhancer activity was greater when the SNP6 G allele was present compared to the A allele. Thus, for both Guam neurologic disorders and PSP, SNP6 may be the site, or at least one of the sites that determines disease risk, as opposed to some other close marker in LD with SNP6. This hypothesis is strengthened by the observation that even though the high-risk SNP6 allele is the same in the Chamarro as in other populations, the high-risk haplotype in the Chamarro population does not appear to be the H1c haplotype, previously reported to be associated with other neurological diseases (36). In fact, despite the higher frequency of ALS/PDC, the H1c haplotype appears to be much rarer in this population than in populations of European descent, which is inconsistent with a major role of H1c as a contributor to risk of ALS/PDC.

In our study, genotypes at SNP9 interact with SNP6 genotypes to increase risk. SNP9 is a non-synonymous change in exon 6, which is a coding exon. This exon is alternatively spliced and is present in approximately 20–40% of transcripts in the hippocampus and cerebellum, and approximately 10% of transcripts in the cortex (49). However, exon 6 sequences are not present in the aggregated pathologic tau. Thus, it is not clear at this point whether SNP9 functions in a regulatory fashion, or if it simply marks some other polymorphic site that is the true functional polymorphism. The regulation of *MAPT* expression is certainly complex. In addition to the enhancer sequence noted above, mutations that affect the regulation of alternative splicing have a profound effect on disease risk (29,30,50). Thus SNPs 6 and 9 may be in two different regulatory regions of *MAPT*. The fact that the genotypes interact suggests a *cis*-acting mechanism.

A novel finding of our work is that there is a second region marked by SNP2 that is 5′ to *MAPT* and that acts independently of sites within *MAPT* to confer risk. Unlike SNPs 6 and 9, for SNP2, the G allele acts by a dominant mechanism. There are several possible hypotheses as to how SNP2 could influence risk for Guam disease. Perhaps, the most likely hypothesis is that SNP2 or an SNP in LD with SNP2 is in a *cis*-acting regulatory sequence that influences *MAPT* expression. Another related hypothesis is that SNP2 is in LD with polymorphic site in this region that influences the expression of another gene, provisionally called antisense to *MAPT* (*aMAPT*). This gene is transcribed in the opposite direction as *MAPT* and *IMP5*, has a transcription start site in *MAPT* intron 0, and extends past *IMP5* (Fig. 1). *aMAPT* has multiple alternatively spliced forms with one exon overlapping with exon 0 of *MAPT*. This gene may act as a natural antisense regulatory sequence that controls *MAPT* expression (Ian D'Souza, personal communication). It is not clear at present whether the *aMAPT* sequence is translated into a protein. Thus, polymorphic sites 5′ to *MAPT* could influence

Table 4. Univariate logistic regression models of the risk of GD, PDC-G, or ALS-G associated with variants among chromosome 17 H1 homozygotes on Guam

SNP	Genotype	Controls *n*(%)	GD *n*(%)	OR (95% CI)	$P^* > \chi^2_{2df}$	PDC-G *n*(%)	OR (95% CI)	$P^* > \chi^2_{2df}$	ALS-G *n*(%)	OR (95% CI)	$P^* > \chi^2_{2df}$	Global P^{**}
2	A/A	94 (44.3)	42 (30.9)	Referent	0.040	30 (24.2)	Referent	0.001	16 (32.6)	Referent	0.306	0.013
	G/A	90 (42.5)	73 (53.7)	1.82 (1.13–2.93)***		70 (56.5)	2.44 (1.45–4.08)***		26 (53.1)	1.70 (0.85–3.37)		
	G/G	28 (13.2)	21 (15.4)	1.68 (0.86–3.29)		24 (19.4)	2.69 (1.36–5.32)***		7 (14.3)	1.47 (0.55–3.93)		
	A/A	94 (44.3)	42 (30.9)	Referent		30 (24.2)	Referent		16 (32.6)	Referent		
	G/–	118 (55.7)	94 (69.1)	1.78 (1.13–2.81)***		94 (75.8)	2.50 (1.53–4.08)***		33 (67.3)	1.64 (0.85–3.17)		
6	A/A	53 (24.8)	56 (41.2)	Referent	0.006	53 (42.7)	Referent	0.003	19 (38.8)	Referent	0.112	0.009
	A/G	119 (55.6)	60 (44.1)	0.48 (0.29–0.78)***		51 (41.1)	0.43 (0.26–0.71)***		20 (40.8)	0.47 (0.23–0.95)***		
	G/G	42 (19.6)	20 (14.7)	0.45 (0.23–0.86)***		20 (16.1)	0.48 (0.25–0.92)***		10 (20.4)	0.66 (0.28–1.58)		
	G/–	161 (75.2)	80 (58.8)	Referent		71 (57.3)	Referent		30 (61.2)	Referent		
	A/A	53 (24.8)	56 (41.2)	2.13 (1.34–3.37)***		53 (42.7)	2.27 (1.41–3.64)***		19 (38.8)	1.92 (1.00–3.70)***		
7	A/A	70 (33.0)	66 (48.5)	Referent	0.012	61 (49.2)	Referent	0.013	21 (42.9)	Referent	0.306	0.038
	G/A	112 (52.8)	52 (38.2)	0.49 (0.31–0.79)***		48 (38.7)	0.49 (0.30–0.80)***		20 (40.8)	0.60 (0.30–1.18)		
	G/G	30 (14.2)	18 (13.2)	0.64 (0.32–1.25)		15 (12.1)	0.57 (0.28–1.17)		8 (16.3)	0.89 (0.35–2.23)		
	G/–	142 (67.0)	70 (51.5)	Referent		63 (50.8)	Referent		28 (57.1)	Referent		
	A/A	70 (33.0)	66 (48.5)	1.91 (1.23–2.97)***		61 (49.2)	1.96 (1.25–3.09)***		21 (42.9)	1.52 (0.81–2.87)		
9	C/C	61 (28.6)	59 (43.4)	Referent	0.017	52 (42.6)	Referent	0.033	19 (38.8)	Referent	0.348	0.079
	T/C	110 (51.6)	58 (42.6)	0.55 (0.34–0.88)***		49 (40.2)	0.52 (0.32–0.86)***		23 (46.9)	0.67 (0.34–1.33)		
	T/T	42 (19.7)	19 (14.0)	0.47 (0.24–0.90)***		21 (17.2)	0.59 (0.31–1.11)		7 (14.3)	0.54 (0.21–1.39)		
	T/–	152 (71.4)	77 (56.6)	Referent		70 (57.4)	Referent		30 (61.2)	Referent		
	C/C	61 (28.6)	59 (43.4)	1.91 (1.22–3.00)***		52 (42.6)	1.85 (1.16–2.95)***		19 (38.8)	1.58 (0.83–3.01)		

*Model χ^2 for logistic regression of disease status on the three genotype categories for each SNP.
**Fisher's exact test of global genotype frequency differences among chromosome 17 H1 homozygotes in the four diagnosis groups.
***P-value$\leq$0.05 for the effect of the given genotype compared to the referent group estimated using logistic regression.

Table 5. Risk of GD, PDC-G or ALS-G associated with *MAPT* region variants on Guam

MAPT SNP effects	GD OR (95% CI)	PDC-G OR (95% CI)	ALS-G OR (95% CI)	GD, PDC-G or ALS-G OR (95% CI)
2	1.61 (1.00–2.62)	2.16 (1.28–3.66)	1.49 (0.74–3.00)	1.76 (1.18-2.60)
6	0.97 (0.49–1.93)	0.85 (0.42–1.73)	0.66 (0.23–1.93)	0.87 (0.50–1.52)
9	1.06 (0.57–1.97)	0.83 (0.42–1.63)	0.60 (0.21–1.67)	0.88 (0.53–1.46)
6 and 9	3.02 (1.10–8.25)	4.04 (1.40–11.64)	6.80 (1.44–32.14)	3.79 (1.64–8.78)

Analysis was restricted to H1 homozygotes which were 211 controls, 136 GD, 122 PDC-G and 49 ALS-G cases with non-missing genotypes.

αMAPT expression, which in turn would influence *MAPT* expression. Another hypothesis is that the gene product of *IMP5* is involved in Guam disease pathogenesis. SNP2 is a non-synonymous (H303R) change in the potential coding region of *IMP5*, a gene predicted from a number of unspliced expressed sequences in public databases. The predicted amino acid sequence for *IMP5* has strong homology to signal peptide peptidases and weaker homology to presenilin1 and 2 (*PSEN1* and *PSEN2*) (51). Because mutations in *PSEN1* and *PSEN2* cause AD, which is a tauopathy, variability at SNP2 could alter the function of *IMP5* and thus influence risk for Guam disease. *PSEN1* and *PSEN2* are components of a transmembrane protease that causes the γ-secretase cleavage of amyloid precursor protein (APP). This cleavage contributes to the production of an APP fragment called Aβ, which is the primary component of the amyloid plaques in AD. Mutations in *PSEN1* or *PSEN2* alter the γ-secretase cleavage site resulting in a more toxic form of Aβ. However, this hypothesis seems unlikely for the following reasons. First, Aβ deposition is not a feature of ALS-G or PDC-G. Second, there is no data available on whether *IMP5* transcripts are translated to produce a protein. Third, *IMP5* is not strongly homologous to the presenilins. Fourth, the active site aspartates in *IMP5* are in opposite orientation to the presenilins making it unlikely that *IMP5* would cleave APP and thus would not be involved in Aβ production (51). Thus, it is more likely that the risk allele of SNP2 or another SNP in LD with SNP2 influences the regulation of *MAPT* and thus influences the disease process.

The SNP alleles described here are not likely to cause ALS-G, PDG-G or GD, but rather increase risk in combination with other genetic and environmental factors. This conclusion is based on the fact that not all affected subjects have the high-risk alleles, and not all carriers of the high-risk allele have the disease. Also, an earlier analysis of a component of a large pedigree from the village of Umatac found evidence against linkage of *MAPT* and ALS-G/PDC-G (32). The drop in prevalence of ALS-G and the increase in onset ages for both ALS-G and PDC-G over the past few decades suggest a change in exposure to an unknown environmental factor(s), and are not consistent with outbreeding diluting a genetic factor(s). Dietary BMAA (27,52) found in cycad seeds is one candidate for an environmental toxin. Our finding that picking, processing and eating cycads elevate risk for Guam disease (Borenstein, Mortimer, Dahlquist, Wu, Salmon, Gamst, Olichney, Thal, Silbert, Kaye, Adonay, Craig, Schellenberg and Galasko, submitted for publication) supports the hypothesis that BMAA may be an environmental susceptibility factor that potentially interacts with *MAPT* region alleles to increase risk for Guam disease. However, attempts to model neurodegeneration in animals by feeding BMAA-containing flour derived from cycad seeds, as prepared by Chamorros in Guam, required unrealistically large doses to produce an effect (53–55). A major environmental change in Guam is the post-World War II improvement in general diet. Perhaps, comparison of the environment in Guam to that of the Kii peninsula of Japan, where a cluster of very similar familial ALS and PDC cases occurs (21–25) will help identify common environmental and genetic factors.

The work presented here is the first genetic study of GD. Our working hypothesis is that GD is a variation of the same disease as ALS-G and PDC-G, and that the symptoms observed are more a function of when onset occurs rather than the underlying genetic and environmental architecture of these disorders. The fact that the same pattern of risk is observed for multiple SNPs for GD, ALS-G and PDC-G argues for a common disease mechanism involving tau. However, the underlying primary genetic architecture and environmental influence for each of these three Guam disorders is not known and could still be distinct for each, even though a common neurodegenerative pathway is the end result. The *APOE* and *MAPT* region results certainly argue that GD and AD are distinct. In all forms of Guam disease, the ε4 and ε2 *APOE* allele frequencies are not significantly different between cases and controls (Table 2). The remarkably low ε4 frequency for controls (5%, Table 2) is consistent with other Asian populations where the ε4 frequency is typically lower than Caucasian frequencies (56). In almost all AD populations, with few exceptions, ε4 frequencies are elevated relative to controls, even when the control frequency is low (56). In most AD studies to date (57–64), with some exceptions (42,65–69), there appears to be no association between polymorphic sites in *MAPT* and AD. Results from the SNP2 region in AD cohorts have not been described. Arguing against the hypothesis that GD is distinct from AD is that these two disorders are not clinically distinguishable. Additional autopsies for GD cases are needed to establish the relationships between GD and ALS-G, and PDC-G and AD.

The observation that the same SNP (SNP6) influences risk for Guam neurologic disorders and PSP (43) and that other tauopathies such as FTD (37) and CBD (40,41) also show an association with *MAPT* region alleles, argues that these disorders at least partially share a common disease mechanism. The common feature of these diseases is aggregated tau occurring as NFTs, and in the case of PSP, also in glial cells. *MAPT* genetic variation may also play a role in typical Parkinson

disease (PD) (46), which is not a tauopathy. The differences between these disorders are intriguing since the localization of neurodegenerative changes and the associated clinical symptoms vary remarkably between ALS-G, PDC-G, GD, PSP, PD and CBD. Presumably, the difference is the result of other unknown environmental and genetic factors, though the difference could also be due to the interactions between genetic variations in the *IMP5* region versus variation within *MAPT*.

METHODS

Subjects

The Chamorro subjects included in this study were recruited through a series of studies in Guam. Archival clinical data and DNA samples were obtained from the National Institutes of Neurological and Communicative Disorders and Stroke Intramural Research program in Guam (1956–83, Ralph Garruto) and from Kiyomitsu Oyanagi. Diagnoses of ALS and PDC were confirmed by examination of case records including autopsy reports, which were available on many patients. More recently, subjects in Guam were evaluated through the University of Guam–University of California, San Diego Consortium (1995–2006) as part of an NIH Program Project Grant. All subjects (or proxies in the case of demented patients who lacked decisional capacity) provided written informed consent to participate in the study, and the study was approved by Institutional Review Boards at the University of Guam, UCSD and University of Washington. Details regarding subject recruitment and medical evaluation were described previously (12). Briefly, all subjects were first evaluated by medical history, physical examination, and cognitive testing using the Cognitive Abilities Screening Instrument (CASI). Subjects who failed the CASI (cutoff score $\leq$75/100) or with a history or screening physical examination suggestive of neurologic disease underwent a further structured neurological examination that included the Unified Parkinson Disease Rating Scale, a standardized psychometric test battery, and blood tests. Neuroimaging with head CT or MRI was obtained when possible. Consensus diagnoses were made by 3 neurologists after reviewing all relevant information and using standard clinical diagnostic criteria wherever possible. The diagnosis of PDC required insidious onset and gradual progression of primary parkinsonism and dementia, either of which could be the initial feature. However, the onset of parkinsonism during mild-to-moderate stage of dementia was necessary to diagnose PDC. Parkinsonism first noted in patients with severe or end-stage dementia was considered a secondary feature of GD. Dementia was diagnosed using the Diagnostic and Statistical Manual, fourth edition (DSM-IV) criteria (American Psychiatric Association, 1994). The pure dementia syndrome in Guam resembled AD clinically, and many patients met the NINCDS/ADRDA criteria for probable AD (70). Patients with this dementia profile who had additional factors such as stroke and depression met criteria for possible AD. Controls were subjects without any neurologic disorder or dementia. Subjects classified as controls had a CASI score $\geq$80, were functionally independent, and lacked motor weakness, tremor or gait difficulty on a brief screening exam. Subjects with a CASI score $<$80 were classified as controls only if detailed neurological and psychometric evaluation showed no evidence of dementia, mild cognitive impairment or any neurological disorder.

Polymorphic loci and genotyping

Genomic DNA was isolated either from available frozen brain tissue or fresh blood samples from case and control subjects. *APOE* genotypes were determined by a modification of the method of Hixson and Vernier (71). Some SNPs in the *MAPT* region were genotyped as restriction-fragment-length polymorphisms (Table 1). For these loci, short DNA fragments containing the polymorphic sites were produced by polymerase chain amplification (PCR), digested with the appropriate restriction enzyme, the resulting fragments resolved using agarose gel electrophoresis, and fragments visualized with ethidium bromide. Locus del-in9 is an insertion/deletion polymorphism. PCR products spanning this locus differ by 238 bp depending on the presence or absence of the insertion. Size differences were observed using agarose gel electrophoresis. The remaining SNPs were genotyped using TaqMan allele discrimination assays (Applied Biosystems, CA, USA) (Table 1). SNPs were selected after initially screening 18 SNPs in a panel of 16 Chamorro controls (Supplementary Material, Table S2). SNPs were selected as follows. The del-in9 polymorphism was selected because it is a tagging site for the H1/H2 haplotype. SNPs 1 and 2 in genes *CRHR1* and *IMP5*, respectively, were selected to follow-up previous work that showed that polymorphism CA3662 is associated with ALS-G and PDC-G (32), because these SNPs had minor allele frequencies in Chamorros $>$5%, and based on LD, provided non-redundant information. SNPs 3–9 in *MAPT* were selected based on work by others on the association between *MAPT* alleles and PSP (35,43,44), and because these SNPs had minor allele frequencies of $>$5% in a panel of 16 Chamorro controls.

Statistical analysis

A χ^2 goodness-of-fit test was used to assess departure from Hardy–Weinberg equilibrium of the genotype frequencies at each SNP in controls and cases. Pairwise LD between SNPs was measured by estimating $|D'|$, the normalized disequilibrium coefficient (72) and the squared correlation coefficient r^2. Fisher's exact test was used to perform global tests to detect allele or genotype frequency differences across three or more groups. Odds ratios (ORs) and 95% CIs were estimated using logistic regression. All analyses were conducted using Stata 9.1 (StataCorp LP, College Station, TX, USA).

To identify potentially interesting SNPs, we performed global tests of allele and genotype frequency differences among the four diagnosis groups (controls, ALS-G, PDC-G and GD). Global tests allow multiple groups to be compared using a single statistical test, thereby protecting against inflated false-positive rates due to multiple comparisons. A global significance level of ~10% was used to select SNPs for more detailed comparisons of the controls and each case group separately. Disease-specific models of the combined effects of multiple SNPs were constructed using